

DOT/FAA/ES-83/3

Systems Engineering
Service
Washington, D.C. 20591

The IF-77 Electromagnetic Wave Propagation Model

G. D. Gierhart
and
M. E. Johnson
U.S. Department of Commerce
National Telecommunications and Information Administration
Institute for Telecommunications
Boulder, Colorado 80303

September 1983

Final Report

This document is available to the U.S. public
through the National Technical Information
Service, Springfield, Virginia 22161.



U.S. Department of Transportation
Federal Aviation Administration

1. Report No. DOT/FAA/ES-83/3		2. Government Accession No.		3. Recipient's Catalog No.	
4. Title and Subtitle The IF-77 Electromagnetic Wave Propagation Model				5. Report Date September 1983	
				6. Performing Organization Code	
				8. Performing Organization Report No.	
7. Author(s) G. D. Gierhart and M. E. Johnson				10. Work Unit No. (TRAIS)	
9. Performing Organization Name and Address U.S. Dept. of Commerce National Telecommunications & Information Administration Institute for Telecommunication Sciences ITS.S3 325 Broadway Boulder, CO 80303				11. Contract or Grant No. DTFA01-82-Y-10539	
				13. Type of Report and Period Covered Final	
12. Sponsoring Agency Name and Address U.S. Dept. of Transportation Federal Aviation Administration Systems Engineering Service Washington, D. C. 20591				14. Sponsoring Agency Code AES-520	
				15. Supplementary Notes FAA Frequency Engineering Branch, AES-520	
16. Abstract This report provides a description of the computational details in the IF-77 (ITS-FAA-1977) radio wave propagation model. The IF-77 model is useful in estimating service coverage for radio systems operating in the 0.1 to 20 GHz frequency range. It is applicable to many air/air, air/ground, air/satellite, ground/ground, and ground/satellite systems. Irregular terrain and propagation beyond the line-of-sight range are considered in the model. However, the terrain feature is keyed to the lower (or facility) antenna and the radio horizon for the upper (or aircraft) antenna is (1) determined from the facility horizon obstacle (common horizon) or (2) taken as the smooth earth radio horizon when a common horizon is negated by the earth's bulge. Previous publications concerning IF-77 include (1) an applications guide for computer programs that use IF-77, (2) an extensive comparison of predictions made using IF-77 with measured data, and (3) an atlas of propagation curves applicable to aeronautical systems. Details concerning the computer programs are not included in this report.					
17. Key Words air/air, air/ground, earth/satellite, propagation model, protection ratio, transmission loss			18. Distribution Statement This document is available to the U. S. public through the National Technical Information Service, Springfield, VA 22161		
19. Security Classif. (of this report) UNCLASSIFIED		20. Security Classif. (of this page) UNCLASSIFIED		21. No. of Pages 89	22. Price

English/Metric Conversion Factors

Length

From \ To	Cm	m	Km	in	ft	s mi	nmi
Cm	1	0.01	1×10^{-5}	0.3937	0.0328	6.21×10^{-6}	5.39×10^{-6}
m	100	1	0.001	39.37	3.281	0.0006	0.0005
Km	100,000	1000	1	39370	3281	0.6214	0.5395
in	2.540	0.0254	2.54×10^{-5}	1	0.0833	1.58×10^{-5}	1.37×10^{-5}
ft	30.48	0.3048	3.05×10^{-4}	12	1	1.89×10^{-4}	1.64×10^{-4}
S mi	160,900	1609	1.609	63360	5280	1	0.8688
nmi	185,200	1852	1.852	72930	6076	1.151	1

Area

From \ To	Cm ²	m ²	Km ²	in ²	ft ²	S mi ²	nmi ²
Cm ²	1	0.0001	1×10^{-10}	0.1550	0.0011	3.86×10^{-11}	5.11×10^{-11}
m ²	10,000	1	1×10^{-6}	1550	10.76	3.86×10^{-7}	5.11×10^{-7}
Km ²	1×10^{10}	1×10^6	1	1.55×10^9	1.08×10^7	0.3861	0.2914
in ²	6.452	0.0006	6.45×10^{-10}	1	0.0069	2.49×10^{-10}	1.88×10^{-10}
ft ²	929.0	0.0929	9.29×10^{-8}	144	1	3.59×10^{-8}	2.71×10^{-8}
S mi ²	2.59×10^{10}	2.59×10^6	2.590	4.01×10^9	2.79×10^7	1	0.7548
nmi ²	3.43×10^{10}	3.43×10^6	3.432	5.31×10^9	3.70×10^7	1.325	1

Volume

From \ To	Cm ³	Liter	m ³	in ³	ft ³	yd ³	fl oz	fl pt	fl qt	gal
Cm ³	1	0.001	1×10^{-6}	0.0610	3.53×10^{-5}	1.31×10^{-6}	0.0338	0.0021	0.0010	0.0002
liter	1000	1	0.001	61.02	0.0353	0.0013	33.81	2.113	1.057	0.2642
m ³	1×10^6	1000	1	61,000	35.31	1.308	33,800	2113	1057	264.2
in ³	16.39	0.0163	1.64×10^{-5}	1	0.0006	2.14×10^{-5}	0.5541	0.0346	2113	0.0043
ft ³	28,300	28.32	0.0283	1728	1	0.0370	957.5	59.84	0.0173	7.481
yd ³	765,000	764.5	0.7646	46700	27	1	25900	1616	807.9	202.0
fl oz	29.57	0.2957	2.96×10^{-5}	1.805	0.0010	3.87×10^{-5}	1	0.0625	0.0312	0.0078
fl pt	473.2	0.4732	0.0005	28.88	0.0167	0.0006	16	1	0.5000	0.1250
fl qt	946.3	0.9463	0.0009	57.75	0.0334	0.0012	32	2	1	0.2500
gal	3785	3.785	0.0038	231.0	0.1337	0.0050	128	8	4	1

Mass

From \ To	g	Kg	oz	lb	ton
g	1	0.001	0.0353	0.0022	1.10×10^{-6}
Kg	1000	1	35.27	2.205	0.0011
oz	28.35	0.0283	1	0.0625	3.12×10^{-5}
lb	453.6	0.4536	16	1	0.0005
ton	907,000	907.2	32,000	2000	1

Temperature

$$^{\circ}\text{C} = 9/5 (^{\circ}\text{F} - 32)$$

$$^{\circ}\text{F} = 5/9 (^{\circ}\text{C}) + 32$$

TABLE OF CONTENTS

	<u>PAGE</u>
1. INTRODUCTION	1
2. PROPAGATION MODEL	2
2.1 Transmission Loss	3
2.2 Power Available	6
2.3 Power Density	6
2.4 Desired-to-Undesired Signal Ratios	7
3. HORIZON GEOMETRY	8
3.1 Smooth-Earth Horizons	9
3.2 Facility Horizon	13
3.3 Aircraft (Or Higher Antenna) Horizon	17
4. DIFFRACTION REGION	19
4.1 Rounded-Earth Diffraction	20
4.2 Knife-edge Diffraction	25
4.3 Diffraction Attenuation, A_d	26
5. LINE-OF-SIGHT REGION	27
5.1 Two-Ray Path Length Difference Geometry	27
5.2 Effective Reflection Coefficient	31
5.2.1 Divergence and Ray Length Factors	31
5.2.2 Surface Roughness Factors	32
5.2.3 Counterpoise Factors	34
5.2.4 Antenna Pattern Gain Factors	36
5.2.5 Plane-Earth Reflection Coefficients	40
5.3 Line-of-Sight Transition Distance, d_0	42
5.4 Line-of-Sight Attenuation, A_{LOS}	44
6. SCATTER REGION	45
7. TERRAIN ATTENUATION, A_T	50
8. FREE SPACE LOSS, L_{bf}	50
9. ATMOSPHERIC ABSORPTION	51
10. VARIABILITY	54
10.1 Long-Term Power Fading, $Y_e(q)$	54
10.1.1 Time Blocks	57
10.1.2 Climates	57
10.2 Surface Reflection Multipath	59
10.3 Tropospheric Multipath	60
10.4 Rain Attenuation	62

	<u>PAGE</u>
10.5 Ionospheric Scintillation	64
10.6 Mixing Distributions	64
11. SUMMARY	66

LIST OF FIGURES

FIGURE 1. COMPUTATIONAL FLOW DIAGRAM FOR $L(q)$.	5
FIGURE 2. INPUT ANTENNA HEIGHTS AND SURFACE ELEVATIONS FOR IF-77.	10
FIGURE 3. EFFECTIVE HEIGHT GEOMETRY.	11
FIGURE 4. FACILITY RADIO HORIZON GEOMETRY.	14
FIGURE 5. LOGIC FOR FACILITY HORIZON DETERMINATION.	17
FIGURE 6. GEOMETRY FOR AIRCRAFT RADIO HORIZON.	18
FIGURE 7. PATHS USED TO DETERMINE DIFFRACTION ATTENUATION LINE.	19
FIGURE 8. SPHERICAL EARTH GEOMETRY.	28
FIGURE 9. GEOMETRY FOR DETERMINATION OF EARTH REFLECTION DIFFRACTION PARAMETER, v_g , ASSOCIATED WITH COUNTERPOISE SHADOWING.	35
FIGURE 10. GEOMETRY FOR DETERMINATION OF COUNTERPOISE REFLECTION DIFFRACTION PARAMETER, v_c , ASSOCIATED WITH THE LIMITED REFLECTING SURFACE OF THE COUNTERPOISE.	35
FIGURE 11. SKETCH ILLUSTRATING ANTENNA GAIN NOTATION AND CORRESPONDENCE BETWEEN RAY TAKE-OFF ANGLES AND GAINS.	36
FIGURE 12. GEOMETRY ASSOCIATED WITH ATMOSPHERIC ABSORPTION CALCULATIONS.	52
APPENDIX. ABBREVIATIONS, ACRONYMS, AND SYMBOLS	67
REFERENCES	87

1. INTRODUCTION

Assignments for aeronautical radio in the radio frequency spectrum must be made so as to provide reliable services for an increasing air traffic density [17]¹. Potential interference between facilities operating on the same or on adjacent channels must be considered in expanding present services to meet future demands. Service quality depends on many factors, including signal strength and the desired-to-undesired signal ratio at the receiver. These parameters vary with receiver location and time even when other parameters, such as antenna gain and radiated powers, are fixed.

In 1973, an air/ground propagation model developed at the Department of Commerce Boulder Laboratories (DOC-BL) by the Institute for Telecommunication Sciences (ITS) for the Federal Aviation Administration (FAA) was documented in detail [14]. This IF-73 (ITS-FAA-1973) propagation model has evolved into the IF-77 (ITS-FAA-1977) model, which is applicable to air/air, air/ground, air/satellite, ground/ground, and ground/satellite paths. The IF-77 has been incorporated into a number of computer programs that are useful in estimating the service coverage of radio systems operating in the frequency band from 0.1 to 20 GHz. These programs may be used to obtain a wide variety of computer-generated microfilm plots [19,20]. Extensive comparisons of IF-77 predictions with measured data have been made [21], and an atlas of basic transmission loss predictions was generated using the model [8,22].

The previously published documentation for IF-77 covered only the extensions [15] made to IF-73 and relied on IF-73 documentation [14] to cover most of the model. This approach was used to highlight the extensions and simplify the documentation process. However, an integrated description of the model is needed to give potential users a better understanding of the overall model. Such a description is provided in this report. Although most of the previous descriptions are repeated here in an integrated form, some items are simply referenced. Details concerning computer programs are not included, but it is anticipated that such detail for a few specific programs will be made available in later reports.

Except where otherwise indicated, all equations provided here are dimensionally consistent; e.g., all lengths in a particular equation are expressed in the same units. Distances and heights are always in kilometers, angles always are in radians, and frequency is always in megahertz. In Section 2.3, wavelength is in meters, else-

¹References are listed alphabetically by author at the end of the report so that reference numbers do not appear sequentially in the text.

where it is in kilometers. Braces are used around parameter dimensions when particular units are called for or when a potential dimension difficulty exists. A list of symbols is provided in the appendix.

2. PROPAGATION MODEL

The IF-77 propagation model is applicable to air/ground, air/air, ground/satellite, and air/satellite paths. It can also be used for ground/ground paths that are line-of-sight or smooth earth. Model applications are restricted to telecommunication systems operating at radio frequencies from about 0.1 to 20 GHz with antenna heights greater than 0.5 m. In addition, radio-horizon elevations must be less than the elevation of the higher antenna. The radio horizon for the higher antenna is taken either as a common horizon with the lower antenna or as a smooth earth horizon with the same elevation as the lower antenna effective reflecting plane (Sec. 3.3).

At 0.1 to 20 GHz, propagation of radio energy is affected by the lower, nonionized atmosphere (troposphere), specifically by variations in the refractive index of the atmosphere [1, 2, 3, 4, 6, 9, 18, 23, 30, 33, 34]. Atmospheric absorption and attenuation or scattering due to rain become important at SHF [23, Ch. 8; 28; 34, Ch. 3]. The terrain along and in the vicinity of the great circle path between transmitter and receiver also plays an important part. In this frequency range, time and space variations of received signal and interference ratios lend themselves readily to statistical description [18, 25, 27, 32, 34, Sec. 10].

Conceptually, the model is very similar to the Longley-Rice [26] propagation model for propagation over irregular terrain, particularly in that attenuation versus distance curves calculated for the line-of-sight (Sec. 5), diffraction (Sec. 4), and scatter (Sec. 6) regions are blended together to obtain values in transition regions. In addition, the Longley-Rice relationships involving the terrain parameter Δh are used to estimate radio-horizon parameters when such information is not available from facility siting data (Sec. 3.2). The model includes allowance for:

1. Average ray bending (Sec. 3).
2. Horizon effects (Sec. 3).
3. Long-term power fading (Sec. 10.1).
4. Antenna pattern (elevation only) at each terminal (Sec. 5.2.4).
5. Surface reflection multipath (Sec. 10.2).

6. Tropospheric multipath (Sec. 10.3).
7. Atmospheric absorption (Sec. 9).
8. Ionospheric scintillations (Sec. 10.5).
9. Rain attenuation (Sec. 10.4).
10. Sea state (Sec. 5.2.2).
11. A divergence factor (Sec. 5.2.1).
12. Very high antennas (Sec. 8).
13. Antenna tracking options (Sec. 5.2.4).

Computer programs that utilize IF-77 calculate transmission loss, power available, power density, and/or a desired-to-undesired signal ratio. These parameters are discussed in Sections 2.1 through 2.4. A computational flow chart is provided in Section 2.1 for transmission loss.

2.1 Transmission Loss

Transmission loss has been defined as the ratio (usually expressed in decibels) of power radiated to the power that would be available at the receiving antenna terminals if there were no circuit losses other than those associated with the radiation resistance of the receiving antenna [34, Sec. 2]. Transmission loss levels, $L(q)$, that are not exceeded during a fraction of the time q (or 100 q percent of the time) are calculated from:

$$L(q) = L_b(0.5) + L_{gp} - G_{ET} - G_{ER} - Y_{\Sigma}(q) \quad \text{dB} \quad (1)$$

where $L_b(0.5)$ is the median basic transmission loss [32, Sec. 10.4], L_{gp} is the path antenna gain-loss [26, Sec. 1-3], G_{ET} and G_{ER} are free-space antenna gains for the transmitter and receiver at the appropriate elevation angle, respectively, and $Y_{\Sigma}(q)$ is the total variability from equation 229 of Section 10; i.e.: (229).

Median basic transmission loss, $L_b(0.5)$, is calculated from:

$$L_b(0.5) = L_{br} + A_Y + A_a \quad \text{dB} \quad (2)$$

where L_{br} is a calculated reference level of basic transmission loss, A_Y is a conditional adjustment factor, and A_a is atmospheric absorption from (228) of Section 9. The factor, A_Y , from (243) of Section 10.1, is used to prevent available signal

powers from exceeding levels expected for free-space propagation by an unrealistic amount when the variability about $L_b(0.5)$ is large and $L_b(0.5)$ is near its free-space level.

Free-space basic transmission loss, L_{bf} , from (226) of Section 8, terrain attenuation, A_T , from (221) of Section 7, and a variability adjustment term, $V_e(0.5)$, from (240) of Section 10.1, are used to determine L_{br} ; i.e.:

$$L_{br} = L_{bf} + A_T - V_e(0.5) \quad \text{dB} \quad (3)$$

The value for L_{gp} in (1) is taken as 0 dB in the IF-77 model. This is valid when (a) transmitting and receiving antennas have the same polarization and (b) the maximum antenna gain is less than 50 dB [26, Sec. 1-3].

Values of G_{ET} and G_{ER} for (1) are obtained from $G_{ET} = G_T + G_{NT}$ and $G_{ER} = G_R + G_{NR}$; i.e.:

$$G_{ET,R} = G_{T,R} + G_{NT,R} \quad \text{dBi} \quad (4)$$

where $G_{T,R}$ is the transmitter or receiver main-beam maximum free space antenna gain in decibels greater than isotropic (dBi), and $G_{NT,R}$ is a normalized transmitting or receiving antenna gain in decibels greater than maximum gain that gives relative gain for the appropriate elevation angle. These gains are all model input parameters. Normalized vertical (elevation) antenna patterns are used to define $G_{NT,R}$ so that gain values can be obtained for elevation angles at which the maximum gain is not appropriate. The calculation of these elevation angles is discussed in Section 5.2.4. Horizontal antenna patterns are not usually considered part of the IF-77 model, but an allowance for them can be made by adjusting $G_{T,R}$ values. However, horizontal patterns have been included in one computer program called TWIRL [20, p. 61].

Variabilities associated with long-term power fading, surface reflection multipath, tropospheric multipath, rain attenuation, and ionospheric scintillation are included in $Y_\Sigma(q)$ of (1). These are all discussed in Section 10. Since the adjustment terms associated with long-term power fading are included in the calculation of $L_b(0.5)$, $Y_\Sigma(0.5) = 0$.

A computational flow diagram for $L(q)$ is provided in Figure 1. Although only those equations discussed in this section are included in the diagram, section references are provided for the other calculations involved. Horizon and diffraction

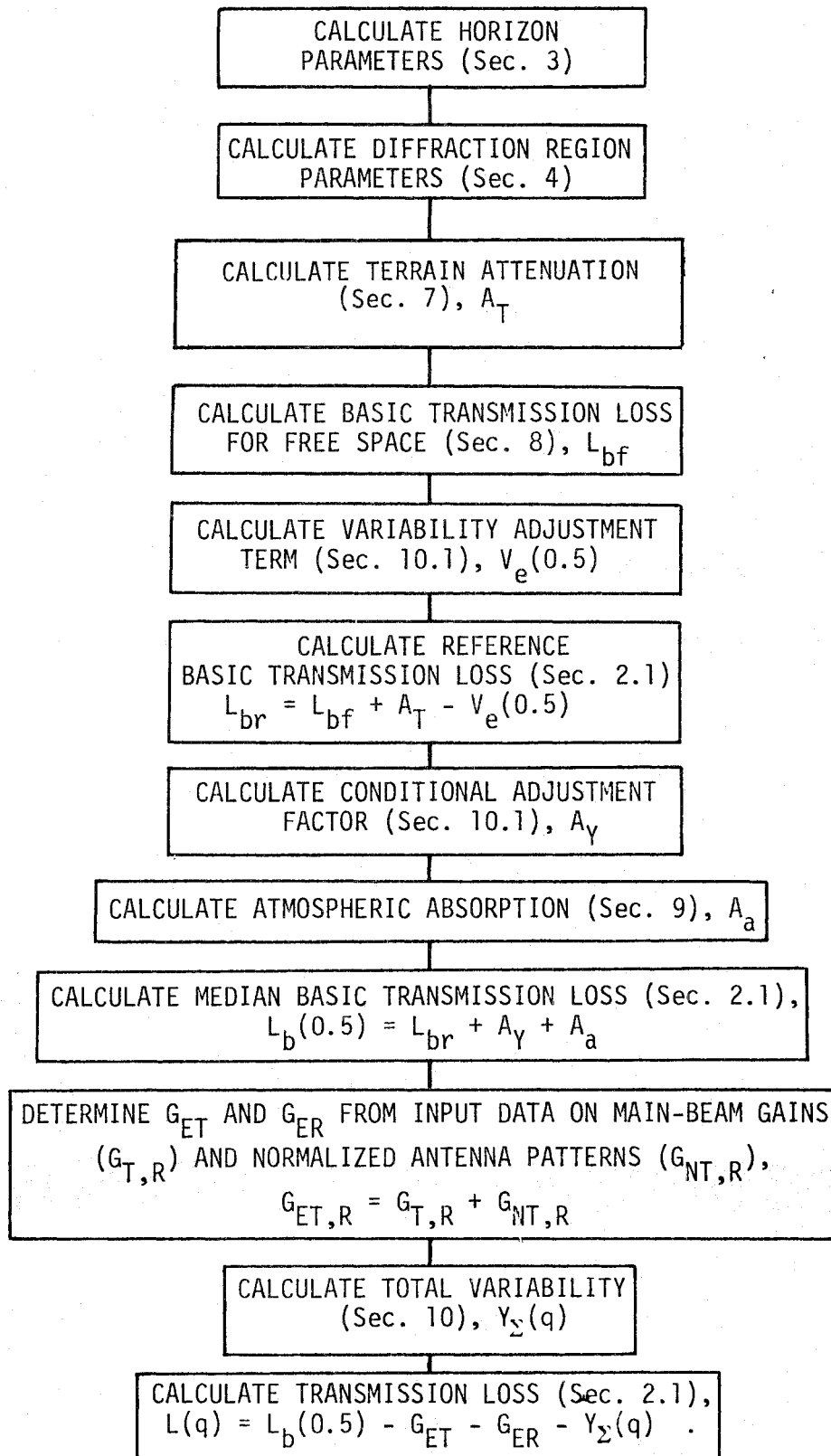


FIGURE 1. COMPUTATIONAL FLOW DIAGRAM FOR $L(q)$.

region parameters are determined prior to calculation of A_T since these parameters are used to define region boundaries.

2.2 Power Available

Power available as calculated in IF-77 is taken as the power available from the receiving antenna terminals under matched conditions when internal heat losses of the receiving antenna and path antenna gain-losses are neglected. Compensation for internal heat loss or gain-loss factors needed to refer the available power to some point in the receiving system other than the receiving antenna terminals can be made by an appropriate adjustment to the radiated power or antenna gains used for computer program input.

Power available $P_a(q)$ levels exceeded for a fraction of time q are determined using $L_b(0.5)$ from (2), $G_{NT,R}$ from (4), and $Y_\Sigma(q)$ from (229) of Section 10 with:

$$P_a(q) = \text{EIRPG} + G_{NT} + G_{NR} - L_b(0.5) + Y_\Sigma(q) \quad \text{dBW} \quad (5)$$

$$\text{EIRPG} = \text{EIRP} + G_R \quad \text{dBW} \quad (6)$$

$$\text{EIRP} = P_{TR} + G_T \quad \text{dBW} \quad (7)$$

Here EIRP is equivalent isotropically radiated power; P_{TR} in decibels greater than 1 W (dBW) is the total power radiated by the transmitting antenna; and $G_{T,R}$ in decibels greater than isotropic (dBi) is the maximum gain of the transmitting antenna or receiving antenna, respectively (Sec. 2.1). Losses (e.g., line losses) associated with the transmitting system should be considered in calculating radiated power from transmitter output power. Normalized antenna gains (G_{NT} and G_{NR}) in decibels greater than maximum gain (G_T or G_R) are included in (5) to allow for antenna directivity when maximum gains are not appropriate (i.e., the antennas are not pointed at each other). Computer programs utilizing IF-77 have tracking options that allow antennas to track each other (Sec. 5.2.4).

2.3 Power Density

Power density $S_R(q)$ in decibels greater than 1 watt per square meter that is exceeded for a fraction of the time q is determined using the parameters discussed previously along with the effective area, A_I , of an isotropic antenna; i.e.:

$$S_R(q) = \text{EIRP} + G_{NT} - L_b(0.5) + Y_\Sigma(q) - A_I \quad \text{dB-W/sq m} \quad (8)$$

Values of A_I are determined from:

$$A_I = 10 \log (\lambda_m^2/4\pi) \quad \text{dB-sq m} \quad (9)$$

where λ_m is the wavelength in meters (33, Sec. 4.11). For a frequency of f [MHz]:

$$\lambda_m = 299.7925/f \quad \text{m} \quad (10a)$$

$$\lambda = \lambda_m/1000 \quad \text{km} \quad (10b)$$

2.4 Desired-to-Undesired Signal Ratio

Desired-to-undesired signal ratios that are available for at least a fraction time q , $D/U(q)$ dB, at the terminals of a lossless receiving antenna are calculated using [11, Sec. 3]:

$$D/U(q) = D/U(0.5) + Y_{DU}(q) \quad \text{dB} \quad (11)$$

The median value of $D/U(0.5)$ and the variability $Y_{DU}(q)$ of D/U are calculated as:

$$D/U(0.5) = [P_a(0.5)]_{\text{Desired}} - [P_a(0.5)]_{\text{Undesired}} \quad (12)$$

$$Y_{DU}(q) = \pm \sqrt{[Y_{\Sigma}(q)]^2_{\text{Desired}} + [Y_{\Sigma}(1-q)]^2_{\text{Undesired}}} \quad \text{dB} \quad (13)$$

- for $q \geq 0.5$

+ otherwise

Values of $P_a(0.5)$ are calculated from (5) where $Y_{\Sigma}(0.5) = 0$ by using parameters appropriate for either the desired or undesired facility. Applicable variabilities are calculated using the methods described in Section 10. Note that $Y_{DU}(q)$ requires the undesired facility Y_{Σ} for $(1 - q)$; e.g.:

$$Y_{DU}(0.8) = - \sqrt{[Y_{\Sigma}(0.8)]^2_{\text{Desired}} + [Y_{\Sigma}(0.2)]^2_{\text{Undesired}}}$$

3. HORIZON GEOMETRY

Calculations associated with horizon geometry involve the use of the effective earth radius concept in which ray bending caused by refraction within the troposphere is simplified by using straight rays above an earth with an effective radius that is selected to compensate for the ray bending [3, Sec. 3.6; 30]. The effective earth radius, a , is calculated [34, Sec. 4] using the minimum monthly mean surface refractivity referred to mean sea level, N_0 , and the height of the effective reflection surface above mean sea level (msl), h_r ; i.e.:

$$N_s = \text{greater of } \left\{ \begin{array}{l} N_0 \exp(-0.1057 h_r) \\ \text{or} \\ 200 \end{array} \right\} \text{ N-units} \quad (14)$$

$$a_0 = 6370 \text{ km} \quad (15)$$

$$a = a_0 [1 - 0.04665 \exp(0.005577 N_s)]^{-1} \text{ km} \quad (16)$$

Here N_s is surface refractivity at the effective reflecting surface, and a_0 is the actual earth radius to three significant figures. Both N_0 [20, p. 74, p. 94] and h_r [20, p. 83] are model input parameters.

When high (>3 km) antennas are involved, geometry based solely on the effective radius method may overestimate ray bending so that smooth earth horizon distances become excessive [31]. This difficulty is compensated for in IF-77 by the use of ray tracing in the determination of some key parameters such as effective terminal altitudes (Sec. 3.1), smooth earth horizon distances (Sec. 3.1), and effective distance (Sec. 10.1). In IF-77, ray tracing is performed through an exponential atmosphere [3, equations 3.43, 3.44, 3.40] in which the refractivity, N , varies with height above msl, h , as:

$$N = N_s \exp[-C_e (h - h_r)] \text{ N-units} \quad (17)$$

where

$$C_e = \log_e \left(\frac{N_s}{N_s + \Delta N} \right) \quad (18)$$

and

$$\Delta N = -7.32 \exp(0.005577 N_s) \text{ N-units/km} \quad (19)$$

Thayer's algorithm [37] for ray tracing through a horizontally stratified atmosphere is used with layer heights (above h_r) taken as 0.01, 0.02, 0.05, 0.1, 0.2, 0.305, 0.5, 0.7, 1, 1.524, 2, 3.048, 5, 7, 10, 20, 30.48, 50, 70, 90, 110, 225, 350, and 475 km. Above 475 km ray bending is neglected; i.e., rays are assumed to be straight relative to a true earth radius, a_0 . The computer subroutine used for ray tracing [14, Sec. B.4.1, RAYTRAC] was written so that: (a) the initial ray elevation angle may be negative; (b) if the initial angle is too negative, it will be set to a value that corresponds to grazing for a smooth earth; and (c) the antenna heights may be very large, e.g., satellites.

The IF-73 model was actually developed for transmission from a ground-based facility to an airborne receiver; but, because of reciprocity, it could also be used for air-to-ground transmissions. Although the IF-77 model does not require that a terminal be ground-based, or that a terminal be airborne, we will nevertheless refer to the lowest terminal as the facility and the higher terminal as the aircraft. Furthermore, the facility is taken as terminal 1 so that variables associated with it have a 1 in their subscripts; and the aircraft is taken as terminal 2.

Horizons for both terminals are determined by the input parameters used to define the facility horizon; i.e., the aircraft horizon is either taken as the facility horizon obstacle (common horizon) or as a smooth earth when the aircraft's view of the facility obstacle would be shadowed by a smooth earth. The calculation of aircraft horizon parameters (Sec. 3.3) involves prior determination of effective antenna heights (Sec. 3.1) and the facility horizon (Sec. 3.2).

3.1 Smooth-Earth Horizons

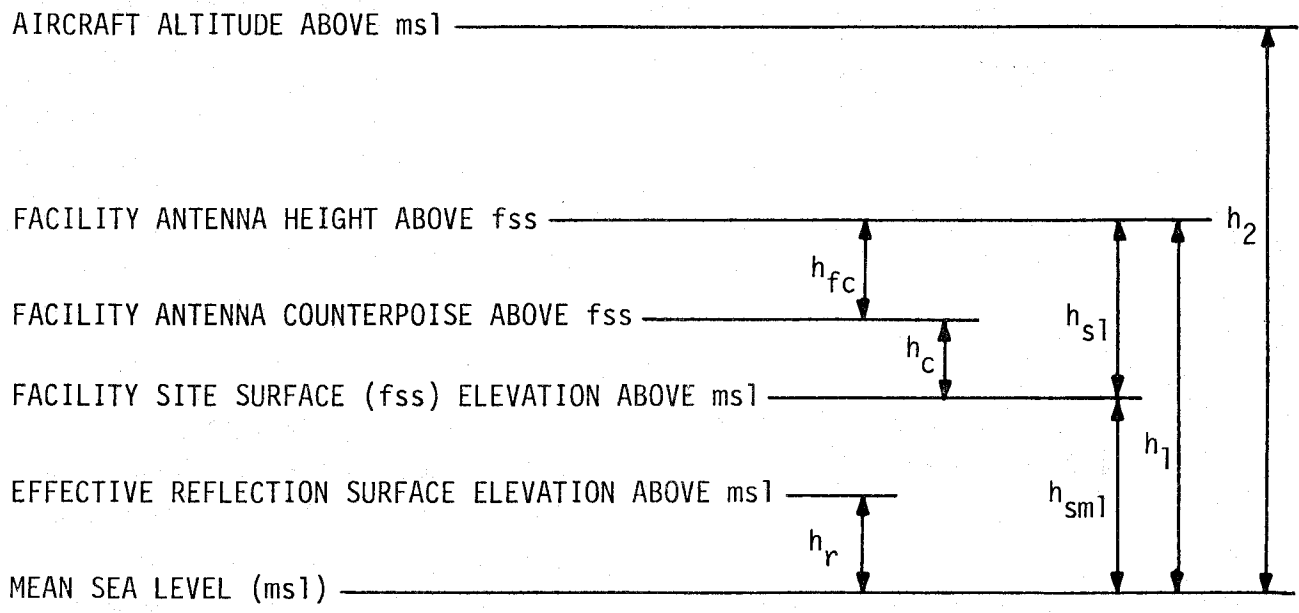
Antenna height information is input to IF-77 via the variables h_r , h_{s1} , h_c , h_{sm1} , and h_2 where these variables are defined in Figure 2 as in the Application Guide [20, pp. 80, 81, 83, 88; 101]. Antenna heights, $h_{r1,2}$, above the effective reflection surface are obtained from these by using:

$$h_{r1} = h_{s1} + h_{sm1} - h_r \quad \text{km} \quad (20a)$$

$$h_{r2} = h_2 - h_r \quad \text{km} \quad (20b)$$

Antenna heights above mean sea level (msl) are given by:

$$h_{1,2} = h_{r1,2} + h_r \quad \text{km} \quad (21)$$



VALID INPUT CONSTRAINTS

- $0 \leq h_r \leq 4 \text{ km}$
- $0 \leq h_{sm1} \leq 4 \text{ km}$
- $0.0005 \text{ km} < h_{s1}$
- $h_1 \leq h_2$

Note that aircraft altitude is elevation above ms1 while the facility antenna height is measured with respect to fss.

FIGURE 2. INPUT ANTENNA HEIGHTS AND SURFACE ELEVATIONS FOR IF-77.

The height of the facility antenna above the counterpoise is given by:

$$h_{fc} = h_{s1} - h_c \quad \text{km} \quad (22)$$

When the effective earth geometry (straight rays) overestimates bending, effective antenna heights, $h_{e1,2}$, are taken as heights that will yield the smooth-earth horizon distances obtained via ray tracing when used with effective earth geometry. As illustrated in Figure 3, effective heights are lower than actual heights.

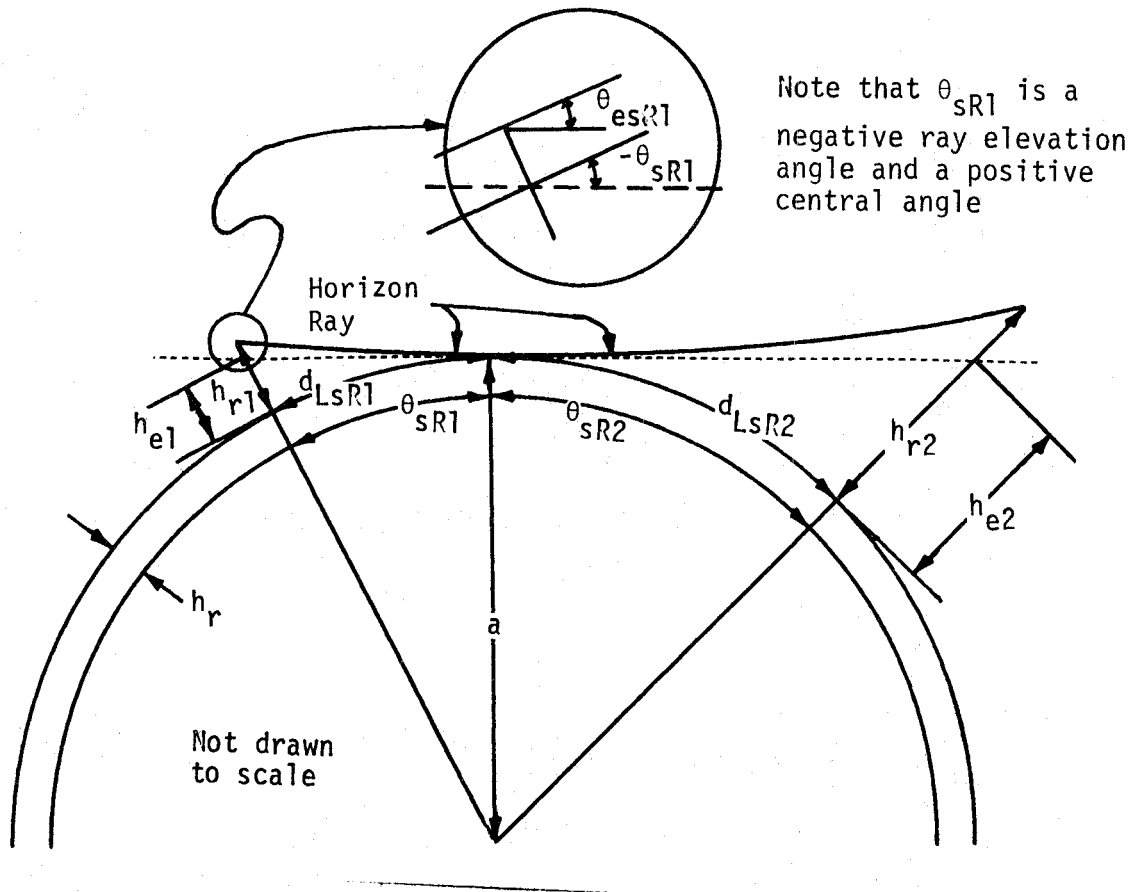


FIGURE 3. EFFECTIVE HEIGHT GEOMETRY.

The IF-77 model uses ray tracing to determine smooth-earth horizon ray distances associated with both terminals, $d_{LSR1,2}$, that are used in the calculation of effective antenna heights. These distances are determined by ray tracing from the effective reflecting surface elevation of the earth's surface to the respective antenna heights. The initial takeoff angle used is 0° and the surface refractivity, N_s , is calculated from N_0 with (14). Values for $d_{LSR1,2}$ and a from (16) are used to determine the difference in actual and effective antenna heights, $\Delta h_{e1,2}$, as follows:

$$\theta_{sR1,2} = d_{LsR1,2}/a \quad \text{rad} \quad (23)$$

$$h_{e1,2} = \text{lesser of } \left[\begin{array}{l} h_{r1,2} \\ \text{or} \\ \left\{ \begin{array}{l} 0.5 d_{LsR1,2}^2/a \text{ if } \theta_{sR1,2} \leq 0.1 \text{ rad} \\ a[\sec(\theta_{sR1,2}) - 1] \text{ otherwise} \end{array} \right\} \end{array} \right] \quad \text{km} \quad (24)$$

$$\Delta h_{e1,2} = h_{r1,2} - h_{e1,2} \quad \text{km} \quad (25)$$

The final value of a smooth earth horizon distance, $d_{Ls1,2}$, is taken as the ray tracing value for high antennas ($\Delta h_{e1,2} > 0$) or computed via effective earth radius geometry, $d_{LsE1,2}$; i.e.:

$$d_{LsE1,2} = \sqrt{2a h_{e1,2}} \quad \text{km} \quad (26)$$

$$d_{Ls1,2} = \left\{ \begin{array}{l} d_{LsR1,2} \text{ if } \Delta h_{e1,2} > 0 \\ d_{LsE1,2} \text{ otherwise} \end{array} \right\} \quad \text{km} \quad (27)$$

$$d_{Ls} = d_{Ls1} + d_{Ls2} \quad \text{km} \quad (28)$$

In addition, the ray elevation angle $\theta_{esR1,2}$ resulting from ray tracing is taken as the final ray elevation angle when $\Delta h_{e1,2} > 0$; i.e.:

$$\theta_{s1,2} = d_{Ls1,2}/a \quad \text{rad} \quad (29)$$

$$\theta_{es1,2} = \left\{ \begin{array}{l} \theta_{esR1,2} \text{ if } \Delta h_{e1,2} > 0 \\ -\theta_{s1,2} \text{ otherwise} \end{array} \right\} \quad \text{rad} \quad (30)$$

3.2 Facility Horizon

The IF-73 model allowed the facility horizon to be specified by: (a) any two horizon parameters (elevation, elevation angle, or distance); (b) estimated with any one horizon parameter and the terrain parameter, Δh ; (c) estimated from Δh alone; or (d) calculated for smooth-earth conditions [14, Fig. 14]. Figure 4 illustrates the facility horizon geometry involved in the IF-73 formulation. Horizon distances, d_{LE1} ; horizon elevation, h_{LE1} ; and horizon elevation angle, θ_{eE1} ; for effective earth geometry are related to each other by:

$$\theta_{eE1} = \tan^{-1} \left(\frac{h_{LE1} - h_1}{d_{LE1}} - \frac{d_{LE1}}{2a} \right) \text{ rad} \quad (31)$$

$$h_{LE1} = h_1 + \frac{(d_{LE1})^2}{2a} + d_{LE1} \tan \theta_{eE1} \text{ km} \quad (32)$$

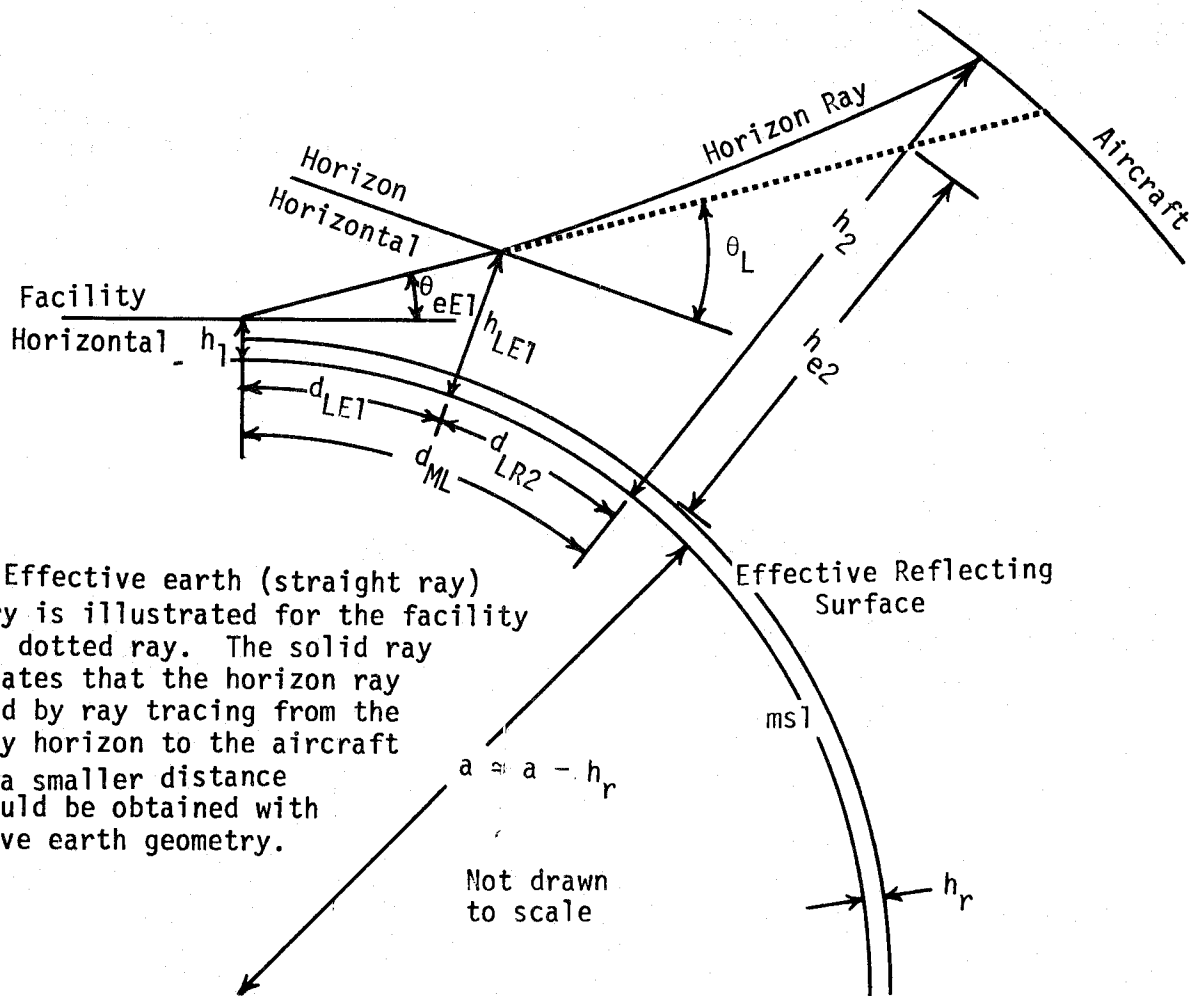
$$d_{LE1} = \pm \sqrt{2a(h_{LE1} - h_1) + a^2 \tan^2 \theta_{eE1}} - a \tan \theta_{eE1} \text{ km} \quad (33)$$

where a is from (16). The \pm choice in (33) is made such that (32) yields its smallest positive value. If d_{LE1} and/or θ_{eE1} are not specified, they may be estimated [26, Sec. 2.4] using Δh [km] which is a model input parameter [20, p. 101] and d_{LS1} from (27). That is:

$$h_e = \text{larger of } (h_{e1} \text{ or } 0.005) \text{ km} \quad (34)$$

$$d_h = d_{LS1} \exp(-0.07 \sqrt{\Delta h/h_e}) \text{ km} \quad (35)$$

$$d_{LE1} = \left\{ \begin{array}{ll} 0.1 d_{LS1} & \text{if } d_h < 0.1 d_{LS1} \\ 3 d_{LS1} & \text{if } d_h > 3 d_{LS1} \\ d_h & \text{otherwise} \end{array} \right\} \text{ km} \quad (36)$$



Note: Effective earth (straight ray) geometry is illustrated for the facility using a dotted ray. The solid ray illustrates that the horizon ray obtained by ray tracing from the facility horizon to the aircraft yields a smaller distance than would be obtained with effective earth geometry.

Not drawn to scale

FIGURE 4. FACILITY RADIO HORIZON GEOMETRY.

$$\theta_{eE1} = \text{lesser of } \left\{ \begin{array}{l} \frac{0.5}{d_{Ls1}} \left[1.3 \left(\frac{d_{Ls1}}{d_{LE1}} - 1 \right) \Delta h - 4h_{e1} \right] \\ \text{or} \\ 0.2094 \quad (12^\circ) \end{array} \right\} \text{ rad} \quad (37)$$

where d_{Ls1} is from (27).

However, some of this flexibility must be sacrificed when the facility is high (airborne) since the accurate specification of more than one horizon parameter requires prior knowledge of ray-tracing results.

The IF-77 version was constructed to retain all of the IF-73 facility horizon specification flexibility for low-facility antennas and, yet, allows ray tracing to be used for high-facility antennas. This method is described in the following steps:

1. Determine horizon parameters as they were determined in IF-73; but, consider the results as initial values that may be changed if the facility antenna is too high.

2. Values of h_1 from (21) and h_{e1} from (24) are used to test the initial horizon parameters. The initial parameter values are replaced by ones appropriate for a smooth earth if the test conditions are met; i.e., smooth-earth values are used if;

$$h_{e1} > 3 \text{ km and } \left\{ \begin{array}{l} \theta_{eE1} > 0 \quad \text{and} \quad h_1 > h_{LE1} \\ \text{or} \\ \theta_{eE1} \leq 0 \quad \text{and} \quad h_1 < h_{LE1} \end{array} \right\}$$

3. Step 3 is not used if smooth earth parameters were selected in step 2. If Δh_{e1} from (25) is zero, the initial horizon parameter values from step 1 are used. Otherwise, ray tracing is used to determine values for θ_{e1} and d_{L1} . In either case:

$$h_{L1} = h_{LE1} \quad (38)$$

$$h_{Lr1} = h_{L1} - h_r \quad (39)$$

$$\theta_{e1} = \left\{ \begin{array}{l} \theta_{eE1} \text{ if } \Delta h_{e1} = 0 \\ \text{otherwise use ray tracing} \end{array} \right\} \quad (40)$$

$$d_{L1} = \left\{ \begin{array}{l} d_{LE1} \text{ if } \Delta h_{e1} = 0 \\ \text{otherwise use ray tracing} \end{array} \right\} \quad (41)$$

The ray tracing referred to in (40) and (41) is started at the horizon elevation, h_{Lr1} , with a take-off angle of $-\theta_L$ and continues until the facility antenna height h_{r1} is reached. Then, the great-circle distance traversed by the ray is taken as d_{L1} ; and the negative of the ray arrival angle is taken as θ_{e1} . The take-off angle used is calculated from:

$$\theta_L = \theta_{eE1} + \left(d_{LE1}/a \right) \quad (42)$$

Figure 5 provides a summary of the logic used for facility horizon determination.

The distance d_{LR2} shown in Figure 4 is taken as the distance under a ray traced from the facility horizon with a take-off angle of θ_L from (42) to the aircraft altitude of h_2 . This distance is then used with $d_{Ls1,2}$ from (27) to calculate the maximum line-of-sight distance d_{ML} which is also shown in Figure 4; i.e.:

$$d_{ML} = \left\{ \begin{array}{l} d_{Ls1} + d_{Ls2} \text{ for smooth earth; i.e., } \Delta h = 0 \\ a \left(\cos^{-1} \left(\frac{(a + h_{e1}) \cos \theta_{e1}}{(a + h_{e2})} \right) - \theta_{e1} \right) \text{ if } \Delta h_{e2} = 0 \\ d_{L1} + d_{LR2} \text{ otherwise} \end{array} \right\} \text{ km} \quad (43)$$

3.3 Aircraft (Or Higher Antenna) Horizon

Aircraft horizon parameters are determined using either (a) case 1, where the facility horizon obstacle is assumed to provide the aircraft radio horizon, or (b) case 2, where the effective reflection surface is assumed to provide the aircraft

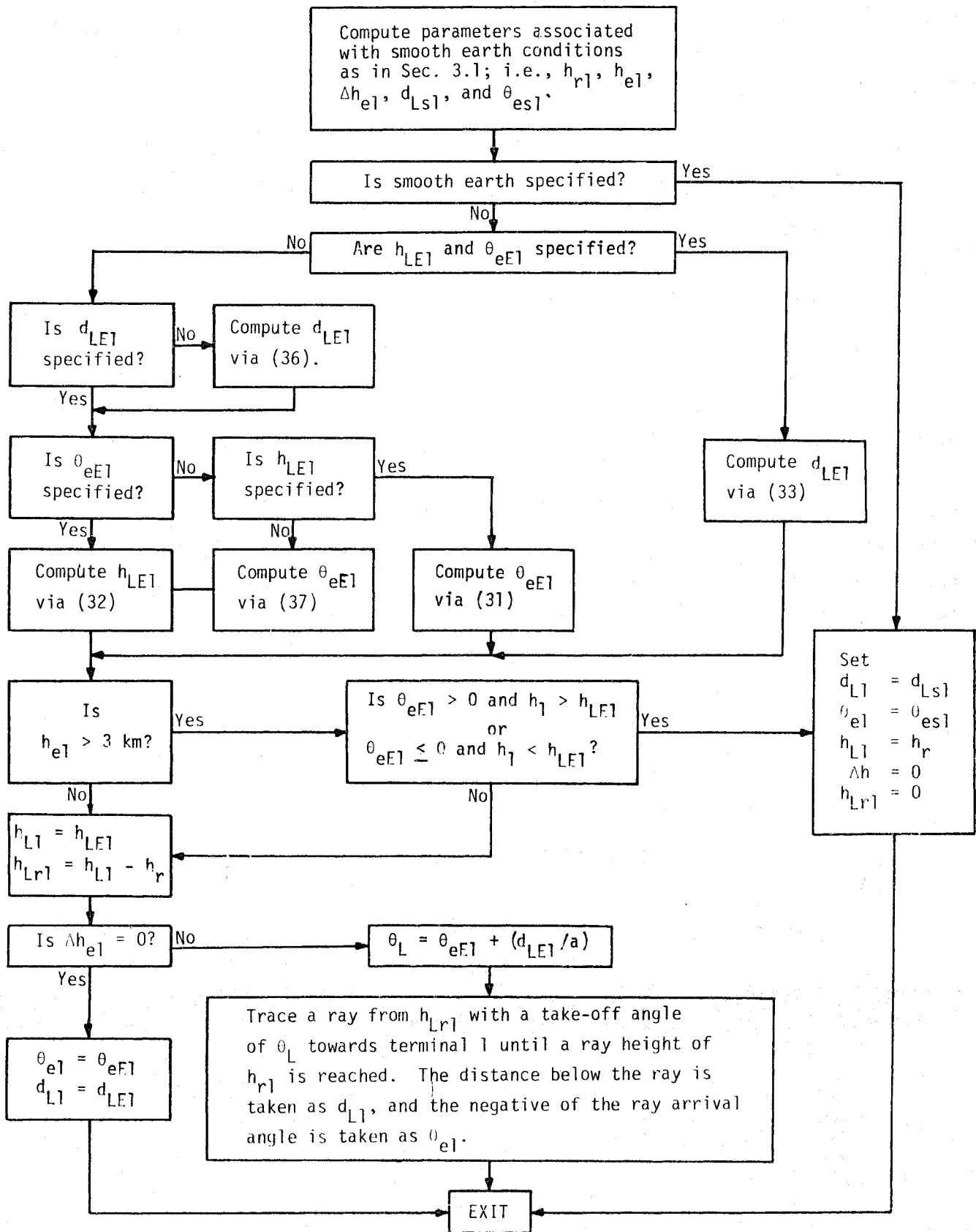


FIGURE 5. LOGIC FOR FACILITY HORIZON DETERMINATION.

with a smooth-earth radio horizon. The great-circle horizon distance for the aircraft, d_{L2} , is calculated using the parameters shown in Figure 6 along with the great-circle distance, d , between the facility and the aircraft; i.e.:

$$d_{sL} = \sqrt{2a h_{Lr1}} \quad \text{km} \quad (44)$$

$$d_{LM} = d_{L1} + d_{sL} + d_{Ls2} \quad \text{km} \quad (45)$$

$$d_{L2} = \left\{ \begin{array}{ll} d - d_{L1} & \text{if } d_{ML} \leq d \leq d_{LM} \\ d_{Ls2} & \text{otherwise} \end{array} \right\} \quad \text{km} \quad (46)$$

Here, h_{Lr1} is the height of the facility horizon obstacle above the effective reflection surface from Figure 5, and d_{sL} is the smooth-earth horizon distance for the obstacle (i.e., a is from (16), d_{L1} is from (41), and d_{Ls2} is from (27)). The horizon ray elevation angle at the aircraft, θ_{e2} , is measured relative to the horizontal at the aircraft, with positive values assigned to values above the horizontal. It is calculated from:

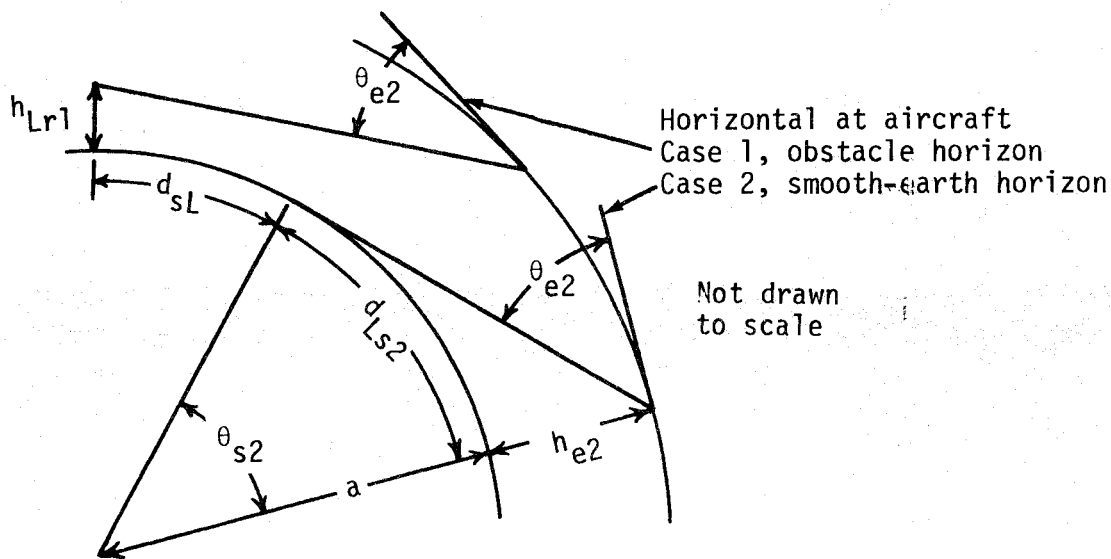


FIGURE 6. GEOMETRY FOR AIRCRAFT RADIO HORIZON

$$h_{Lr2} = \left\{ \begin{array}{l} h_{Lr1} \text{ if } d_{ML} < d < d_{LM} \\ 0 \text{ otherwise} \end{array} \right\} \quad \text{km} \quad (47)$$

$$h_{L2} = h_{Lr2} + h_r \quad \text{km} \quad (48)$$

$$\theta_{e2} = \text{Tan}^{-1} \left(\frac{h_{Lr2} - h_{e2}}{d_{L2}} - \frac{d_{L2}}{2a} \right) \quad \text{rad} \quad (49)$$

where h_{Lr2} is the aircraft horizon height above the reflecting surface.

4. DIFFRACTION REGION

Calculations based on diffraction mechanisms are used both within and beyond the radio horizon. Diffraction attenuation, A_d , is assumed to vary linearly with distance in the diffraction region when other parameters (heights, etc.) are fixed. Most of the equations given in this section are related to the determination of two points needed to define this diffraction line. Since irregular terrain may be involved, rounded-earth diffraction is combined with knife-edge diffraction considerations. This is done by combining attenuation values obtained via rounded earth with those obtained using knife-edge diffraction at two distances (d_{ML} and d_A), and fitting a straight attenuation versus distance line to them. The paths involved may be illustrated using the points shown in Figure 7 as path F-O-ML for d_{ML} and path

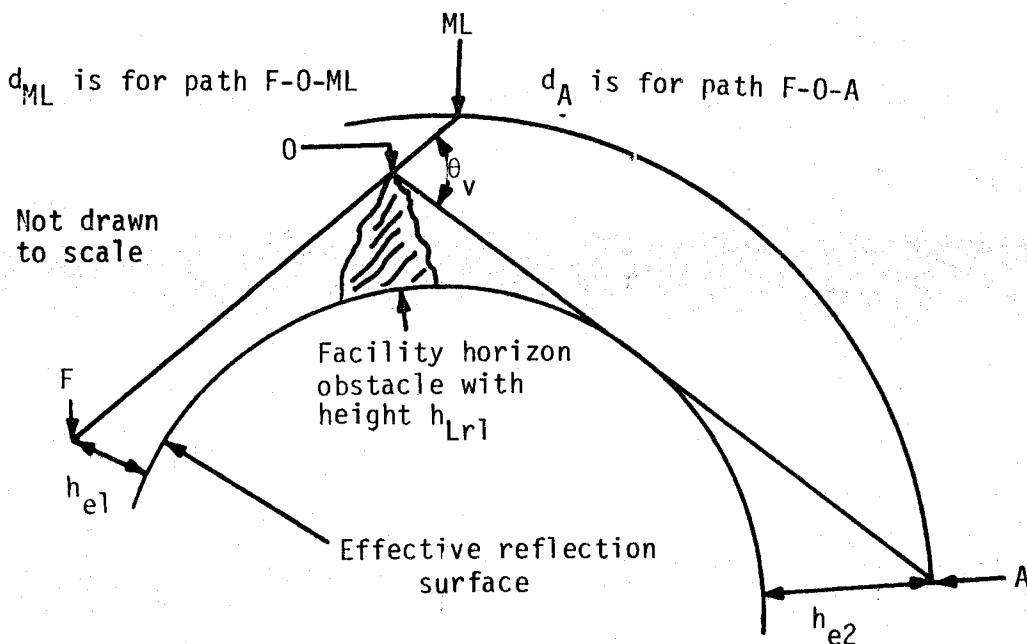


FIGURE 7. PATHS USED TO DETERMINE DIFFRACTION ATTENUATION LINE.

F-0-A for d_A where d_{ML} corresponds to the maximum line-of-sight distance and d_A is the shortest beyond-the-horizon distance that involves both the facility horizon obstacle and a smooth-earth horizon for the aircraft.

Rounded-earth and knife-edge diffraction calculations are discussed in Sections 4.1 and 4.2, respectively. Section 4.3 deals with the determination of the diffraction attenuation, A_d .

4.1 Rounded-Earth Diffraction

Rounded-earth diffraction calculations in IF-77 involve the determination of straight-line attenuation versus distance parameters for paths F-0-ML and 0-A of Figure 7. Key parameters for these calculations are as follows:

$$h_{ep1} = \left\{ \begin{array}{l} h_{e1} \text{ from (24) for path F-0-ML} \\ h_{Lr1} \text{ from (39) for path 0-A} \end{array} \right\} \text{ km} \quad (50)$$

$$h_{ep2} = h_{e2} \text{ km from (24) for both paths} \quad (51)$$

$$d_{Lp1} = \left\{ \begin{array}{l} d_{L1} \text{ from (41) for path F-0-ML} \\ d_{L01} = d_{sL} \text{ from (44) for path 0-A} \end{array} \right\} \text{ km} \quad (52)$$

$$d_{Lp2} = \left\{ \begin{array}{l} d_{ML} - d_{L1} \text{ for path F-0-ML} \\ \quad \text{with } d_{ML} \text{ from (43)} \\ d_{L02} = d_{Ls2} \text{ from (27) for path 0-A} \end{array} \right\} \text{ km} \quad (53)$$

$$A_p = \left\{ \begin{array}{l} \text{Attenuation line intercept} \\ A_F \text{ for path F-0-ML} \\ A_0 \text{ for path 0-A} \end{array} \right\} \text{ dB} \quad (54)$$

$$M_p = \left\{ \begin{array}{l} \text{Attenuation line slope} \\ M_F \text{ for path F-O-ML} \\ M_0 \text{ for path O-A} \end{array} \right\} \quad \text{dB/km} \quad (55)$$

$$G_{\bar{h}p1,2} = \left\{ \begin{array}{l} \text{Height gain function} \\ G_{\bar{h}F1,2} \text{ for path F-O-ML} \\ G_{\bar{h}O1,2} \text{ for path O-A} \end{array} \right\} \quad \text{dB} \quad (56)$$

With appropriate starting parameters from (50) through (53), A_p , M_p , and $G_{\bar{h}p1,2}$ are determined as follows:

a = effective earth radius from (16)

f = frequency [MHz]

$$\theta_3 = 0.5 (a^2/f)^{1/3}/a \quad \text{rad} \quad (57)$$

$$\theta_4 = 3\theta_3 \quad \text{rad} \quad (58)$$

$$d_{Lp} = d_{Lp1} + d_{Lp2} \quad \text{km} \quad (59)$$

$$d_3 = d_{Lp} + a\theta_3 \quad \text{km} \quad (60)$$

$$d_4 = d_3 + 2a\theta_3 \quad \text{km} \quad (61)$$

$$a_{1,2} = d_{Lp1,2}^2 / (2h_{ep1,2}) \quad \text{km} \quad (62)$$

$$a_{3,4} = (d_{3,4} - d_{Lp}) / \theta_{3,4} \quad \text{km} \quad (63)$$

σ = conductivity (Siemens) which is an input parameter
[20, p. 99, SURFACE TYPE OPTIONS]

$$x = 18000 \sigma / f \quad (64)$$

ϵ = dielectric constant which is an input parameter
[20, pp. 99, SURFACE TYPE OPTIONS]

$$K_{d1,2,3,4} = 0.36278 (fa_{1,2,3,4})^{-1/3} [(\epsilon - 1)^2 + x^2]^{-1/4} \quad (65)$$

$$K_{1,2,3,4} = \left\{ \begin{array}{l} K_{d1,2,3,4} \quad \text{for horizontal polarization} \\ \text{or} \\ K_{d1,2,3,4} [\epsilon^2 + x^2]^{1/2} \quad \text{for vertical polarization} \end{array} \right\} \quad (66)$$

$$K_{F1,2} = \text{smaller of } (K_{1,2} \text{ or } 0.99999) \quad (67)$$

$$B_{1,2,3,4} = 416.4f^{1/3}(1.607 - K_{1,2,3,4}) \quad (68)$$

$$X_{1,2} = B_{1,2} a_{1,2}^{-2/3} d_{Lp1,2} \quad \text{km} \quad (69)$$

$$X_{3,4} = B_{3,4} a_{3,4}^{-2/3} (d_{3,4} - d_{Lp}) + X_1 + X_2 \quad \text{km} \quad (70)$$

$$G_{1,2,3,4} = 0.05751 X_{1,2,3,4} - 10 \log X_{1,2,3,4} \quad (71)$$

$$W_{1,2} = 0.0134 X_{1,2} \exp(-0.005 X_{1,2}) \quad (72)$$

$$y_{1,2} = 40 \log (X_{1,2}) - 117 \quad \text{dB} \quad (73)$$

$$F_{1,2} = \left\{ \begin{array}{l} y_{1,2} \text{ or } -117 \text{ whichever has the smaller absolute} \\ \text{value for } 0 \leq K_{F1,2} \leq 10^{-5} \\ \text{or} \\ y_{1,2} \text{ for } 10^{-5} \leq K_{F1,2} \text{ and} \\ \quad -450 \left(\log K_{F1,2} \right)^{-3} \leq X_{1,2} \\ \text{or} \\ 20 \log (K_{F1,2}) - 15 + 2.5 (10^{-5}) X_{1,2}^2 / K_{F1,2} \\ \text{otherwise} \end{array} \right\} \quad \text{dB} \quad (74)$$

$$F_{X1,2} = \left\{ \begin{array}{l} F_{1,2} \text{ for } 0 \leq X_{1,2} \leq 200 \\ \text{or} \\ W_{1,2} y_{1,2} + (1 - W_{1,2}) G_{1,2} \text{ for } 200 < X_{1,2} < 2000 \\ \text{or} \\ G_{1,2} \text{ for } 2000 < X_{1,2} \end{array} \right\} \text{ dB} \quad (75)$$

$$A_{3,4} = G_{3,4} - F_{X1} - F_{X2} - 20 \text{ dB} \quad (76)$$

$$M_p = (A_4 - A_3)/(d_4 - d_3) \text{ dB/km} \quad (77)$$

$$A_p = A_4 - M_p d_4 \text{ dB} \quad (78)$$

$$B_{N1,2} = 1.607 - K_{1,2} \quad (79)$$

$$\bar{h}_{1,2} = 2.235 B_{N1,2}^2 (f^2/a_{1,2})^{1/3} h_{ep1,2} \quad (80)$$

$$f_{c1,2} = 0.3 \sqrt{d_{Lp1,2}^\lambda} \quad (81)$$

where λ is from (10b):

$$G_{W1,2} = \left\{ \begin{array}{l} 0 \text{ if } h_{ep1,2} \geq 2 f_{c1,2} \\ 1 \text{ if } h_{ep1,2} \leq f_{c1,2} \\ \text{or} \\ 0.5 \left(1 + \cos \left(\frac{\pi(h_{ep1,2} - f_{c1,2})}{f_{c1,2}} \right) \right) \\ \text{otherwise} \end{array} \right\} \quad (82)$$

$$\left. \begin{array}{l}
\text{Whenever } h_{ep1,2} \geq 2 f_{c1,2} \\
0 \\
\text{or when } \bar{h}_{1,2} \geq 2.5 \\
-6.6 - 0.013 \bar{h}_{1,2} - 2 \log \bar{h}_{1,2} \\
\text{or when } K_{1,2} \leq 0.01 \\
1.2 - 13.5 \bar{h}_{1,2} + 15 \log \bar{h}_{1,2} \quad \text{if } \bar{h}_{1,2} < 0.3 \\
-6.5 - 1.67 \bar{h}_{1,2} + 6.8 \log h_{1,2} \quad \text{if } \bar{h}_{1,2} \geq 0.3 \\
\text{or when } 0.01 < K_{1,2} \leq 0.05 \\
T - 25 (T - B) (0.05 - K_{1,2}) \\
\text{where} \\
T = -13.9 + 24.1 \bar{h}_{1,2} + 3.1 \log \bar{h}_{1,2} \quad \text{if } \bar{h}_{1,2} < 0.25 \\
T = -5.9 - 1.9 \bar{h}_{1,2} + 6.6 \log \bar{h}_{1,2} \quad \text{if } \bar{h}_{1,2} \geq 0.25 \\
B = 1.2 - 13.5 \bar{h}_{1,2} + 15 \log \bar{h}_{1,2} \quad \text{if } \bar{h}_{1,2} < 0.3 \\
B = -6.5 - 1.67 \bar{h}_{1,2} + 6.8 \log \bar{h}_{1,2} \quad \text{if } \bar{h}_{1,2} \geq 0.3 \\
\text{or when } K_{1,2} > 0.05 \\
T - 20 (T - B) (0.1 - K_{1,2}) \\
\text{where} \\
T = -13 \text{ if } \bar{h}_{1,2} < 0.1 \\
T = -4.7 - 2.5 \bar{h}_{1,2} + 7.6 \log \bar{h}_{1,2} \quad \text{if } \bar{h}_{1,2} \geq 0.1 \\
B = -13.9 + 24.1 \bar{h}_{1,2} + 3.1 \log \bar{h}_{1,2} \quad \text{if } \bar{h}_{1,2} < 0.25 \\
B = -5.9 - 1.9 \bar{h}_{1,2} + 6.6 \log \bar{h}_{1,2} \quad \text{if } \bar{h}_{1,2} \geq 0.25
\end{array} \right\} \text{dB} \quad (83)$$

$$G_{hp1,2} = \left(G_{hl,2} \right) \left(G_{wl,2} \right) \quad \text{dB} \quad (84)$$

Note that many of the variables used in (60) through (84) have values that are dependent upon path parameters from (50) through (56), but are not identified with a p subscript.

The formulation provided in (83) for $G_{\bar{h}_{1,2}}$ is based on a curve fit approximation to the residual height gain function curves [34, Fig. 7.2] developed by A. G. Longley of NTIA (unpublished paper, "Calculation of Transmission Loss for Frequencies from 200 MHz to 10 GHz"). While this approximation may yield incorrect values for $K_{1,2} > 0.1$, $\bar{h}_{1,2} < 0.01$ km or $\bar{h}_{1,2} > 100$ km, the application of the height-gain function in many such cases should be tempered anyway. Although special consideration for the $K_{1,2} > 0.1$ and $\bar{h}_{1,2} < 0.01$ km cases are not included in (83), the initial test of $h_{ep1,2}$ against $2f_{c1,2}$ will result in $G_{\bar{h}_{1,2}} = 0$ for almost all cases where $\bar{h}_{1,2} > 100$ km. Furthermore, the abrupt $G_{\bar{h}_{1,2}}$ change associated with this test is tempered by the "blending function" of (82) in (84) [24, eq. 6].

Rounded-earth diffraction attenuation for the path F-0-A, A_{rF} , is given by:

$$A_{rF} = A_F + M_F d \quad \text{dB} \quad (85)$$

and the rounded-earth diffraction attenuation for path 0-A at distance $d_{L01} + d_{L02}$, A_{r0} , is:

$$A_{r0} = A_0 + M_0(d_{L01} + d_{L02}) \quad \text{dB} \quad (86)$$

4.2 Knife-Edge Diffraction

Knife-edge diffraction attenuation by an isolated obstacle with ground reflections [24, Sec. 3.5; 34, Sec. 7.2] is calculated for the F-0-M and F-0-A paths [34; Sec's. 7.2, III.3] illustrated in Figure 7; i.e., $A_{KML,A}$. These calculations utilize $G_{\bar{h}_{F1,2}}$ and $G_{\bar{h}_{01}}$ from (56) and (84), $d_{L01,2}$ from (52,53), θ_{e1} and d_{L1} from Figure 5, θ_{es2} from (30), a from (16), A_{r0} from (86), d_{ML} from (43), and frequency f [MHz]. That is:

$$A_{KML} = 6 - G_{\bar{h}_{F1}} - G_{\bar{h}_{F2}} \quad \text{dB} \quad (87)$$

$$d_{LSA} = d_{L01} + d_{L02} \quad \text{km} \quad (88)$$

$$\theta_v = \theta_{e1} + \theta_{es2} + (d_{L1} + d_{LsA})/a \quad \text{rad} \quad (89)$$

$$v = 5.1658 \sin(0.5\theta_v) \sqrt{fd_{L1}d_{LsA}/(d_{L1} + d_{LsA})} \quad (90)$$

$$C_v = \int_0^v \cos\left(\frac{\pi t^2}{2}\right) dt, \quad S_v = \int_0^v \sin\left(\frac{\pi t^2}{2}\right) dt \quad (91)$$

where these are Fresnel integrals [34, p. III-18].

$$f_v = 0.5 \sqrt{[1 - (C_v + S_v)]^2 + (C_v - S_v)^2} \quad (92)$$

$$A_{KA} = A_{r0} - G_{hF1} - G_{h01} - 20 \log f_v \quad \text{dB} \quad (93)$$

4.3 Diffraction Attenuation, A_d

Diffraction attenuation, A_d , is calculated using the rounded-earth diffraction (Sec. 4.1) and knife-edge diffraction (Sec. 4.2) parameters just discussed; i.e.

$$W = \left\{ \begin{array}{l} 1 \text{ when } d_{ML} \geq d_{Ls} \text{ (rounded-earth only)} \\ 0 \text{ when } d_{ML} \leq 0.9 d_{Ls} \text{ (knife-edge only)} \\ 0.5 \left(1 + \cos\left(\frac{\pi(d_{Ls} - d_{ML})}{0.1 d_{Ls}}\right) \right) \text{ otherwise} \\ \text{(combination of both)} \end{array} \right\} \quad (94)$$

where the maximum line-of-sight distance, d_{ML} , is from (43), and the total smooth-earth horizon distance, d_{Ls} , is from (28):

$$A_{ML} = \left\{ \begin{array}{l} A_{rML} \text{ if } W > 0.999 \\ A_{KML} \text{ if } W < 0.001 \\ (1 - W) A_{KML} + W A_{rML} \text{ otherwise} \end{array} \right\} \quad \text{dB} \quad (95)$$

where $A_{rML} = A_{rF}$ from (85) with $d = d_{ML}$ and A_{KML} is from (87).

$$d_A = d_{L1} + d_{LsA} \quad \text{km} \quad (96)$$

d_A is the facility-to-aircraft distance of Figure 7, d_{L1} is from Figure 5, and d_{LSA} is from (88).

$$A_A = \left\{ \begin{array}{l} A_{rA} \text{ if } W > 0.999 \\ A_{KA} \text{ if } W < 0.001 \\ (1 - W) A_{KA} + W A_F \text{ otherwise} \end{array} \right\} \text{ dB} \quad (97)$$

where $A_{rA} = A_{rF}$ from (85) with $d = d_A$ and A_{KA} is from (93).

$$M_d = (A_{ML} - A_A) / (d_{ML} - d_A) \quad \text{dB/km} \quad (98)$$

$$A_{d0} = A_{ML} - M_d d_{ML} \quad \text{dB} \quad (99)$$

$$A_d = A_{d0} + M_d d \quad \text{dB} \quad (100)$$

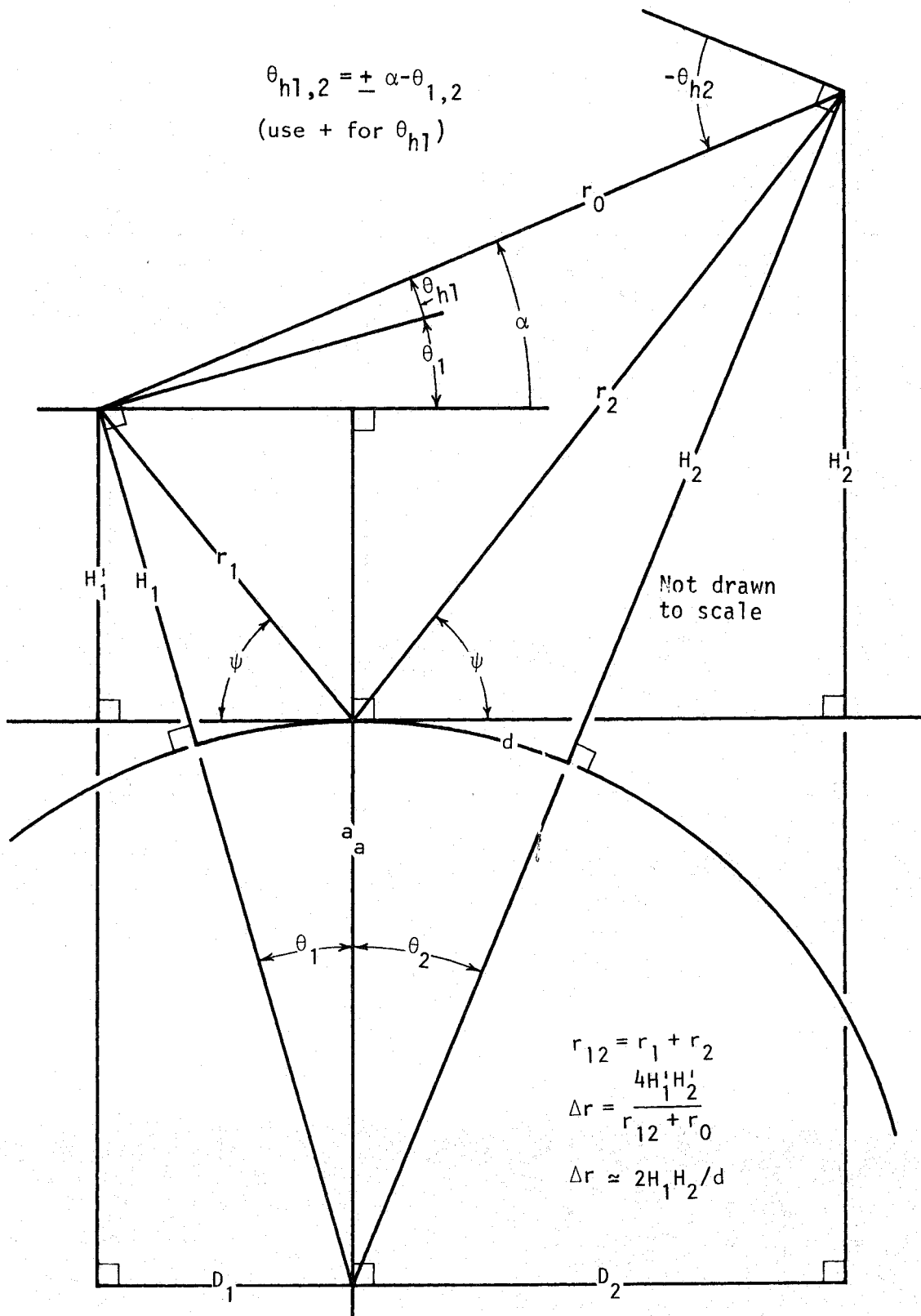
where d [km] is the great-circle path distance and A_d is the diffraction attenuation applicable to it. The use of A_d in the determination of terrain attenuation, A_T , is discussed in Section 7.

5. LINE-OF-SIGHT REGION

Calculations based on a two-ray model are used in estimating an attenuation, A_{LOS} (Sec. 5.4), and short-term fading statistics, Y_π (Sec. 10.2), for paths with distances less than the maximum line-of-sight (LOS) range, d_{ML} from (43). This model involves the phasor summation of the earth reflected and direct rays. The geometry and effective reflection coefficient associated with it are discussed in Sections 5.1 and 5.2, respectively. At distances less than d_{ML} but greater than the LOS transition distance, d_0 (Sec. 5.3), diffraction makes a contribution to A_{LOS} .

5.1 Two-Ray Path Length Difference Geometry

Geometry for the two-ray model used in the LOS region is shown in Figure 8. Path length difference, Δr , is the extent by which the length of the reflected ray path, $r_1 + r_2 = r_{12}$, exceeds that of the direct ray r_0 ; i.e.:



Note: Relationships between the various geometric parameters shown here were previously provided in IF-73 [14, Sec. A.4.2].

FIGURE 8. SPHERICAL EARTH GEOMETRY.

$$\Delta r = r_{12} - r_0 \quad \text{km} \quad (101)$$

The geometrical parameters encountered in the calculation of Δr are used in other parts of the model (e.g., antenna gain factors, Sec. 5.2.4), and Δr is used in the two-ray phasor summation that results in the LOS lobing structure (Sec. 5.4).

The Δr formulation provided here uses a_0 from (15), a from (16), $\Delta h_{e1,2}$ from (25), $h_{r1,2}$ from (20), the height of the counterpoise above ground h_{cg} , and the height of the facility antenna above its counterpoise, h_{fc} . Both h_{cg} and h_{fc} are model input parameters and are used only if the facility counterpoise option is desired. This formulation provides the Δr and path length, d , for a particular grazing angle, ψ ; and it is repeated for various values of ψ until sufficient coverage is obtained for both Δr and d . If a counterpoise is present, a set of calculations will also be required with the counterpoise parameters selected. The formulation may be summarized as follows:

$$z = (a_0/a) - 1 \quad (102)$$

$$k_a = 1/(1 + z \cos \psi) \quad (103)$$

$$a_a = a_0 k_a \quad \text{km} \quad (104)$$

$$\Delta h_{a1,2} = \Delta h_{e1,2} (a_a - a_0)/(a - a_0) \quad \text{km} \quad (105)$$

$$H_1 = \left\{ \begin{array}{l} h_{r1} - \Delta h_{a1} \text{ for earth} \\ h_{fc} \text{ for counterpoise} \end{array} \right\} \quad \text{km} \quad (106a)$$

$$H_2 = \left\{ \begin{array}{l} h_{r2} - \Delta h_{a2} \text{ for earth} \\ h_{r2} - \Delta h_{a2} - h_c \text{ for counterpoise} \end{array} \right\} \quad \text{km} \quad (106b)$$

where h_{fc} is from (22).

$$z_{1,2} = a_a + H_{1,2} \quad \text{km} \quad (107)$$

$$\theta_{1,2} = \cos^{-1} [a_a \cos(\psi)/z_{1,2}] - \psi \quad \text{rad} \quad (108)$$

$$D_{1,2} = z_{1,2} \sin \theta_{1,2} \quad \text{km} \quad (109)$$

$$H'_{1,2} = \left\{ \begin{array}{l} D_{1,2} \tan \psi \text{ for } \psi < 1.56 \text{ rad} \\ H_{1,2} \text{ otherwise} \end{array} \right\} \text{ km} \quad (110)$$

$$\alpha = \left\{ \begin{array}{l} \tan^{-1}[(H'_2 - H'_1)/(D_1 + D_2)] \text{ for } \psi < 1.56 \text{ rad} \\ \psi \text{ otherwise} \end{array} \right\} \text{ km} \quad (111)$$

$$r_o = \left\{ \begin{array}{l} (D_1 + D_2)/\cos \alpha \text{ for } \psi < 1.56 \text{ rad} \\ H_2 - H_1 \text{ otherwise} \end{array} \right\} \text{ km} \quad (112)$$

$$r_{12} = \left\{ \begin{array}{l} (D_1 + D_2)/\cos \psi \text{ for } \psi < 1.56 \text{ rad} \\ H_1 + H_2 \text{ otherwise} \end{array} \right\} \text{ km} \quad (113)$$

$$\Delta r = 4 H'_1 H'_2 / (r_o + r_{12}) \quad \text{km} \quad (114a)$$

$$\Delta r_g = \Delta r \text{ with earth parameters in (106) km} \quad (114b)$$

$$\Delta r_c = \Delta r \text{ with counterpoise parameters in (106) km} \quad (114c)$$

$$\theta_{h1} = \alpha - \theta_1 \quad \text{rad} \quad (115a)$$

$$\theta_{h2} = -(\alpha + \theta_2) \quad \text{rad} \quad (115b)$$

$$\theta_{r1,2} = -(\psi + \theta_{1,2}) \quad \text{rad} \quad (116)$$

$$\theta_o = \theta_1 + \theta_2 \quad \text{rad} \quad (117)$$

$$d = a_a \theta_o \quad \text{km} \quad (118)$$

An adjusted effective earth radius, a_a , and adjusted effective antenna heights, $H_{1,2}$, that vary with ψ are used in this formulation since the values of a from (16), and $h_{r1,2}$ from (20) are not appropriate for large-ray, take-off angles when $\cos \psi$ is not near 1 [3, eq. 3.23]. Since r_0 and r_{12} can be very large and nearly equal, Δr is calculated via (114) instead of (101). Except when the counterpoise case is specifically mentioned, future references to variables calculated in (106) through (118) involve the earth reflection case (e.g., $\Delta r = \Delta r_g$).

5.2 Effective Reflection Coefficient

A counterpoise for the facility antenna (e.g., as with very high frequency omni-range or VOR antenna) is an option of the IF-77 model [20, p. 89]. Hence, reflection coefficients for both earth and counterpoise reflections are computed. Magnitudes for these coefficients are R_{Tg} and R_{Tc} , respectively. The factors involved in these coefficients include the divergence, D_v , and ray-length factors, F_r (Sec. 5.2.1); the surface-roughness factor, $F_{\sigma h}$ (Sec. 5.2.2); counterpoise factors, $f_{g,c}$ (Sec. 5.2.3); antenna gain pattern factors, $g_{Rg,c}$ (Sec. 5.2.4); and plane-earth reflection coefficient magnitudes, $R_{c,g}$ (Sec. 5.2.5); i.e.:

$$R_{Tg} = D_v F_r F_{\sigma h} f_g g_{Rg} R_g \quad (119a)$$

$$R_{Tc} = \left\{ \begin{array}{ll} 0 & \text{when there is no counterpoise} \\ f_c g_{Rc} R_c & \text{otherwise} \end{array} \right\} \quad (119b)$$

Since the counterpoise is taken to be near the facility antenna and flat, $D_v F_r F_{\sigma h}$ is taken as unity in (119b). If there is no counterpoise $f_g = 1$, $R_{Tc} = 0$, and the calculation of f_c , g_{Rc} , and R_c is not done. When isotropic antennas are used, $g_{Rg,c} = 1$.

5.2.1 Divergence and Ray Length Factors

Reflection from the curved earth surface is less efficient than reflection from a flat earth would be [15, Sec. 3.2; 35]. This reduction is taken into account by a divergence factor, D_v , which multiplies the plane-earth reflection coefficients as in (119a).

When both antennas are high and close (i.e., two close aircraft), the relative magnitude of the reflected ray will be reduced because the reflected ray length is much longer than the direct ray length (i.e., larger free space loss for reflected ray) [15, Sec. 3.3]. The ray length factor, F_r , in (119a) is used to account for this.

The formulation for D_v and F_r may be summarized as follows:

$$r_{1,2} = \left\{ \begin{array}{l} H_{1,2} \text{ if } \psi \approx 90^\circ \\ D_{1,2}/\cos \psi \text{ otherwise} \end{array} \right\} \text{ km} \quad (120)$$

where $H_{1,2}$ are from (106); the grazing angle, ψ (Fig. 8), is a starting parameter for the Δr formulation of Section 5.1; and $D_{1,2}$ are from (109)

$$R_r = \frac{r_1 r_2}{r_{12}} \quad \text{km} \quad (121)$$

where $r_{1,2}$ are from (120) and r_{12} is from (113)

$$D_v = \left[1 + \frac{2R_r(1 + \sin^2 \psi)}{a_a \sin \psi} + \left(\frac{2R_r}{a_a} \right)^2 \right]^{-1/2} \quad (122)$$

where a_a is from (104), and

$$F_r = r_0/r_{12} \quad (123)$$

where r_0 is from (112).

5.2.2 Surface Roughness Factors

Surface roughness factors for specular, F_{oh} , and diffuse, F_{doh} , reflections are calculated as follows:

$$\Delta h_d = \Delta h_m [1 - 0.8 \exp(-0.02d)] \quad \text{m} \quad (124)$$

where Δh is the terrain parameter used to characterize irregular terrain and is an IF-77 model input parameter [20, p. 101]; and d is great-circle path distance from (118).

$$\sigma_h = \left\{ \begin{array}{ll} 0.25 H_{1/3} & \text{for water} \\ 0.39 \Delta h_d & \text{for } \Delta h_d \leq 4 \text{ m} \\ 0.78 \Delta h_d \exp(-0.5 \Delta h_d^{1/4}) & \text{otherwise} \end{array} \right\} \text{ m} \quad (125)$$

where $H_{1/3}$ is a value for significant wave height that is selected based on the sea state when a water reflecting surface option is chosen [20, p. 99].

$$\delta = \sigma_h \sin(\psi) / \lambda_m \quad \text{m} \quad (126)$$

where the grazing angle, ψ (Fig. 8), is a starting parameter for the Δr formulation of Section 5.1; and the wavelength in meters, λ_m , is from (10a).

$$F_{\sigma h} = \exp(-2\pi\delta) \quad (127)$$

$$F_{d\sigma h} = \left\{ \begin{array}{ll} 0.01 + 946\delta^2 & \text{if } \delta < 0.00325 \\ 6.15\delta & \text{if } 0.00325 \leq \delta < 0.0739 \\ 0.45 + \sqrt{0.000843 - (\delta - 0.1026)^2} & \text{if } 0.0739 \leq \delta < 0.1237 \\ 0.601 - 1.06\delta & \text{if } 0.1237 \leq \delta < 0.3 \\ 0.01 + 0.875 \exp(-3.88\delta) & \text{otherwise} \end{array} \right\} \quad (128)$$

The formulation for $F_{d\sigma h}$ is based on curves fit to data [5, Fig. 4], and is used along with the plane-earth reflection coefficient magnitude, R_g (Sec. 5.2.5); ray length factor, F_r , from (123); counterpoise factor, f_g (Sec. 5.2.3); and the antenna gain pattern factor, g_{Rg} (Sec. 5.2.4); to formulate the diffuse reflection coefficient; i.e.:

$$R_d = F_r F_{d\sigma h} f_g g_{Rg} R_g \quad (129)$$

5.2.3 Counterpoise Factors

Counterpoise factor, f_g , in (119a) is used to provide some reduction in the reflection from the earth's surface when this reflecting surface is shadowed by the counterpoise. Counterpoise factor, f_c , in (119b) is used to provide some reduction in the reflection from the counterpoise because of the limited area of the counterpoise. When there is no counterpoise, $f_g = 1$ and $f_c = 0$. These factors are determined with the geometry shown in Figures 9 and 10 by using knife-edge diffraction considerations as follows:

$$\theta_{ce} = \tan^{-1}(2 h_{fc}/d_c) \quad \text{rad} \quad (130)$$

where h_{fc} is the height of the facility antenna above its counterpoise from (22), and d_c is the counterpoise diameter which is an IF-77 model input parameter [20, p. 88].

$$r_c = 0.5 d_c / \cos \theta_{ce} \quad \text{km} \quad (131)$$

$$\theta_{kg} = |\theta_{ce}| - |\theta_{r1}| \quad \text{rad} \quad (132)$$

where θ_{r1} is from (116):

$$Y_v = \sqrt{8r_c/\lambda} \quad (133)$$

where λ is from (10b).

$$\theta_{kc} = |\theta_{ce} - \theta_{h1}| \quad \text{rad} \quad (134)$$

where θ_{h1} is calculated using counterpoise parameters in (106) through (118).

$$v_g = \pm Y_v \sin(\theta_{kg}/2) \begin{pmatrix} - & \text{for } |\theta_{r1}| < \theta_{ce} \\ + & \text{otherwise} \end{pmatrix} \quad (135a)$$

$$v_c = \pm Y_v \sin(\theta_{kc}/2) \begin{pmatrix} - & \text{for } \theta_{h1} > \theta_{ce} \\ + & \text{otherwise} \end{pmatrix} \quad (135b)$$

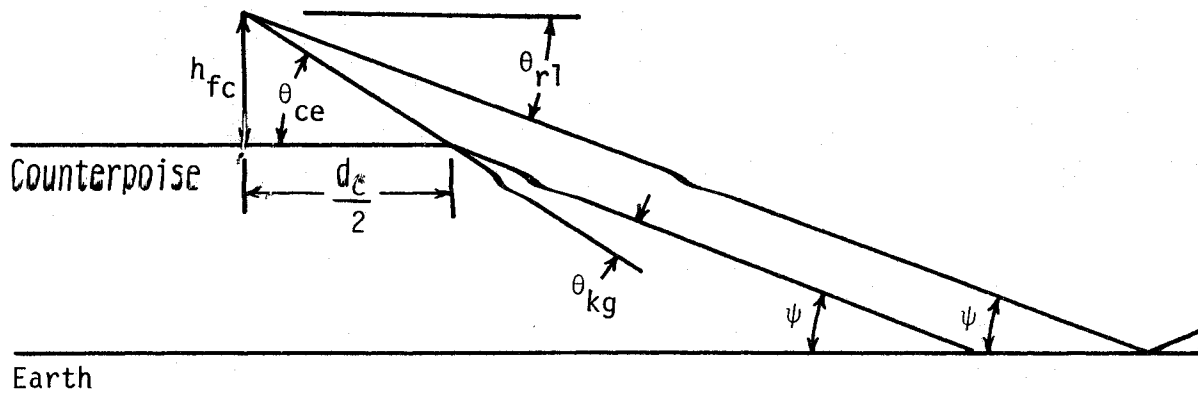


FIGURE 9. GEOMETRY FOR DETERMINATION OF EARTH REFLECTION DIFFRACTION PARAMETER, v_g , ASSOCIATED WITH COUNTERPOISE SHADOWING.

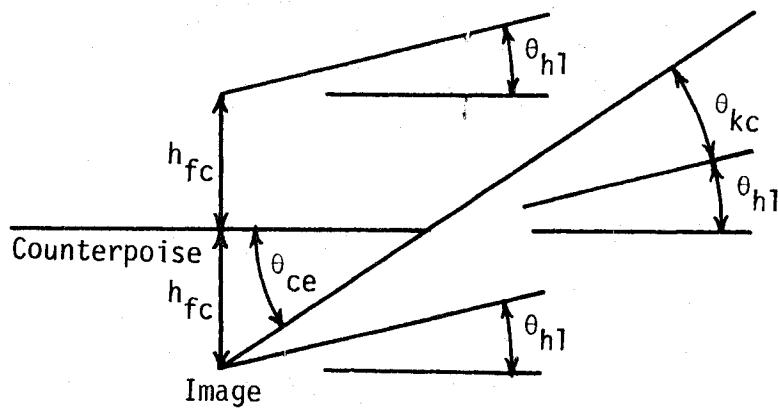


FIGURE 10. GEOMETRY FOR DETERMINATION OF COUNTERPOISE REFLECTION DIFFRACTION PARAMETER, v_c , ASSOCIATED WITH THE LIMITED REFLECTING SURFACE OF THE COUNTERPOISE.

$$C_{g,c} = \int_0^V g_{,c} \cos\left(\frac{\pi t^2}{2}\right) dt, \quad S_{g,c} = \int_0^V g_{,c} \sin\left(\frac{\pi t^2}{2}\right) dt \quad (136)$$

where these are Fresnel integrals [34, p. III-18].

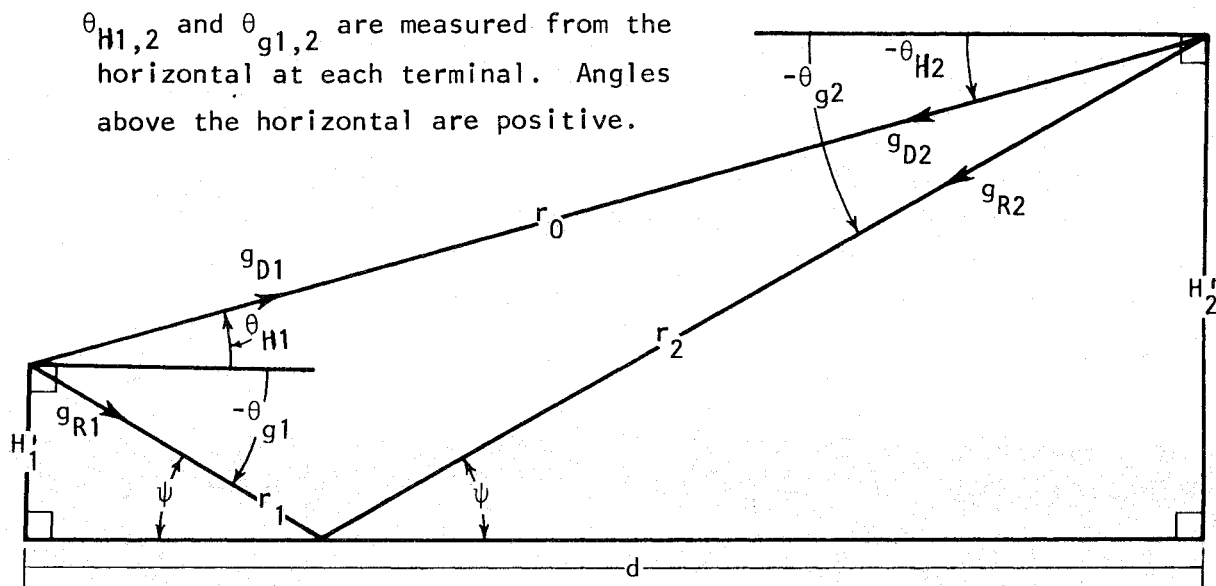
$$f_{g,c} = 0.5 \sqrt{[1 - (C_{g,c} + S_{g,c})]^2 + (C_{g,c} - S_{g,c})^2} \quad (137)$$

$$\phi_{kg,c} = \text{Tan}^{-1}\left(\frac{C_{g,c} - S_{g,c}}{1 - C_{g,c} - S_{g,c}}\right) \text{ rad} \quad (138)$$

The angles $\phi_{kg,c}$ are phase shifts that will be used later in Section 5.4.

5.2.4 Antenna Pattern Gain Factors

The antenna gain factors $g_{D,R}$ and $g_{Rh,v}$ are used to allow for situations where the antenna gains effective for the direct ray path differ from those for the reflected ray path. Figure 11 illustrates the two-ray path and indicates the gains



Note: This sketch is drawn with flat earth, straight rays and an exaggerated scale so that the geometry shown is over simplified.

FIGURE 11. SKETCH ILLUSTRATING ANTENNA GAIN NOTATION AND CORRESPONDENCE BETWEEN RAY TAKE-OFF ANGLES AND GAINS.

involved. These gains are the relative voltage antenna gains (volts/volt or V/V). They are measured relative to the main beam of their respective terminal antennas; i.e., for main beam conditions $g_{D,R} = g_{R1,2} = 1$ V/V. This convention is consistent with usage in IF-73 [14, p. 39]. However, it is NOT CONSISTENT with usage in the Multipath Handbook [16, Sec. CI-D.3] where identical symbols are used; but, the gains are measured relative to an isotropic antenna.

In general, these gains are complex quantities; but, IF-77 includes provisions for scalar gains only; i.e., these gains are >0 and ≤ 1 . In many practical applications, the direct and reflected rays will leave (or arrive) at elevation angles where the relative phase is either expected to be near zero or is unknown so that the complex nature of these gains is largely academic. They are called voltage gains since they are a voltage ratio that could be considered dimensionless (volt/volt), but are different from gains expressed as power ratios (watt/watt) that could also be considered dimensionless. Decibel gains above main beam values are related to these gains by formulas such as:

$$G_{R1,2}[\text{dB}] = 20 \log g_{R1,2} \quad (139)$$

where $G_{R1,2} \leq 0$ because $0 < g_{R1,2} \leq 1$

and

$$g_{R1,2}[\text{V/V}] = 10^{(G_{R1,2}/20)} \quad (140)$$

The formulations for $g_{D,R}$ are:

$$g_D = \left\{ \begin{array}{l} g_{D1}g_{D2} \text{ for linear polarization} \\ 0.5[g_{hD1}g_{hD2} + g_{vD1}g_{vD2}] \text{ for elliptical polarization} \end{array} \right\} \quad (141)$$

$$g_R = \left\{ \begin{array}{l} 1 \text{ for isotropic antennas and/or elliptical} \\ \text{polarization (see text below)} \\ g_{R1}g_{R2} \text{ otherwise} \end{array} \right\} \quad (142)$$

where isotropic implies that, for the radiation angles of interest, $g_{R1} = g_{D1}$ and $g_{R2} = g_{D2}$. In problems involving elliptical polarization, horizontally polarized ($g_{hD1,2}$ and $g_{hR1,2}$) and vertically polarized ($g_{vD1,2}$ and $g_{vR1,2}$) components are used. Linear polarization is considered to be either vertical or horizontal with the polarization associated with $g_{D,R}$ selected accordingly. Defining g_R as 1 for elliptical polarization is done to allow the antenna gains to be included in the reflection coefficient formulation of IF-77 in a simple way for horizontal or vertical polarization. Circular polarization is a special case of elliptical polarization; i.e.,

$$g_{hD1,2} = g_{vD1,2}$$

The gain factor g_{Rv} is similar to g_R except that g_{Rv} involves gains $g_{vR1,2}$; i.e.:

$$g_{Rv}[V/V] = \left\{ \begin{array}{ll} 1 \text{ for isotropic antennas} & \\ g_{vR1}g_{vR2} \quad \text{otherwise} & \end{array} \right\} \quad (143)$$

In a similar manner,

$$g_{Rh}[V/V] = \left\{ \begin{array}{ll} 1 \text{ for isotropic antennas} & \\ g_{hR1}g_{hR2} \quad \text{otherwise} & \end{array} \right\} \quad (144)$$

where g_{Rh} is for horizontal polarization. These factors will be used in the formulation of complex plane-earth reflection coefficients for elliptical polarization that is given in the next section.

Several facility antenna patterns from which gain factors can be determined are included in the computer programs that utilize IF-77 [20, p. 85]. However, data for other facility antenna patterns or aircraft antenna patterns can be used. These programs also include an option to tilt the main beam of either or both antenna(s) relative to the horizontal, or have either or both antenna(s) track the other with its main beam [20, p. 89]. The patterns involved here are vertical plane antenna patterns. Gain variations with azimuth can be accommodated by adjusting $G_{T,R}$ in (4), and $G_{NT,R}$ for (4) are obtained from:

$$G_{NT} = \left\{ \begin{array}{ll} 20 \log g_{D1} & \text{if facility is transmitting} \\ 20 \log g_{D2} & \text{otherwise} \end{array} \right\} \quad (145a)$$

$$G_{NR} = \left\{ \begin{array}{ll} 20 \log g_{D1} & \text{if facility is receiving} \\ 20 \log g_{D2} & \text{otherwise} \end{array} \right\} \quad (145b)$$

The elevation angles to be used in the determination of the various gain factors are listed below:

<u>FACTOR</u>	<u>ELEVATION ANGLE</u>
g_{D1}	θ_{H1} for LOS, otherwise θ_{e1} (Fig. 5)
g_{D2}	θ_{H2} for LOS, otherwise θ_{e2} from (49)
$g_{R1} \cdot g_{VR1} \cdot g_{HR1}$	θ_{g1}
$g_{R2} \cdot g_{VR2} \cdot g_{HR2}$	θ_{g2}

These angles are calculated as follows:

$$\theta_{L1,2} = (\theta_{es1,2} + \theta_{s1,2}) \left(\frac{a_a - a_o}{a - a_o} \right) \quad \text{rad} \quad (146)$$

where $\theta_{es1,2}$ is from (30), $\theta_{s1,2}$ is from (29), a_a is from (104), a_o is from (15), and a is from (16),

$$\theta_{H1,2} = \theta_{h1,2} + \theta_{L1,2} \quad \text{rad} \quad (147)$$

$$\theta_{g1,2} = \theta_{r1,2} + \theta_{L1,2} \quad \text{rad} \quad (148)$$

where $\theta_{h1,2}$ is from (115), and $\theta_{r1,2}$ is from (116). The effect of $\theta_{L1,2}$ is to force $\theta_{H1,2}$ and $\theta_{g1,2}$ to have the values obtained via ray tracing at the smooth-earth horizon, and prorated values obtained elsewhere.

When a counterpoise is present, it will have a set of gain factors associated with it where the earth or counterpoise set values are determined by the values used for $H_{1,2}$ in (106) to calculate $\theta_{h1,2}$ and $\theta_{r1,2}$. For example:

$$g_{Rg} = g_R \text{ calculated with parameters appropriate for a ground reflection} \quad (149a)$$

$$g_{Rc} = g_R \text{ calculated with parameters appropriate for a counterpoise reflection} \quad (149b)$$

5.2.5 Plane-Earth Reflection Coefficients

Values for the plane-earth reflection coefficient, $R \exp(-j\phi)$, are dependent upon the dielectric constant, ϵ , and conductivity, σ , of the surface involved. For water:

$$\epsilon = \frac{\epsilon_s - \epsilon_0}{1 + (2\pi fT)^2} + \epsilon_0 \quad (150)$$

$$\sigma[\text{mho/m}] = \frac{f^2 T (\epsilon - \epsilon_0)}{2865} + \sigma_i \quad (151)$$

where ϵ_s is the static dielectric constant, $\epsilon_0 = 4.9$ is the dielectric constant representing the sum of electronic and atomic polarizations, $f[\text{MHz}]$ is frequency, $T[\mu\text{s}]$ is relaxation time, and $\sigma_i[\text{mho/m}]$ is the ionic conductivity. The values for ϵ_s , T , and σ_i for water [15, p. 26] were obtained using Saxton and Lane [36]. When (150,151) are not used, appropriate ϵ and σ values are taken from the Applications Guide [20, p. 89]. The formulation for $R \exp(-j\phi)$ may be summarized as follows:

$$\epsilon_c = \epsilon - j 60 \lambda_m \sigma \quad (152)$$

where λ_m is from (10a).

$$Y_c = \sqrt{\epsilon_c - \cos^2 \psi} \quad (153)$$

where ψ (Fig. 8) is a starting parameter for the Δr formulation of Section 5.1.

$$R_V \exp[-j(\pi - c_V)] = \frac{\epsilon_c \sin(\psi) - Y_c}{\epsilon_c \sin(\psi) + Y_c} g_R \quad (154a)$$

where g_R is from (142).

$$R_h \exp[-j(\pi - c_h)] = \frac{\sin(\psi) - Y_c}{\sin(\psi) + Y_c} g_R \quad (154b)$$

$$R_e \exp[-j(\pi - c_e)] = 0.5 \{g_{Rh} R_h \exp[-j(\pi - c_h)] + g_{Rv} R_V \exp[-j(\pi - c_V)]\} \quad (154c)$$

where $g_{Rv,h}$ are from (143,144), and

$$R \exp(-j\phi) = \left\{ \begin{array}{l} R_V \exp[-j(\pi - c_V)] \text{ for vertical polarization} \\ \quad \text{(electric field in plane of incidence)} \\ R_h \exp[-j(\pi - c_h)] \text{ for horizontal polarization} \\ \quad \text{(electric field normal to plane of incidence)} \\ R_e \exp[-j(\pi - c_e)] \text{ for elliptical polarization} \end{array} \right\} \quad (155)$$

The part of this formulation for elliptical polarization is valid only when the transmitting and receiving antenna have the same sense and circular polarization is a special case of elliptical polarization.

When earth (or ground) reflection parameters (i.e., gain factors and surface constants) are used in (150) through (155), the resulting reflection coefficient is taken as $R_g \exp(-j\phi_g)$; and, when counterpoise parameters are involved, the resulting coefficient is $R_c \exp(-j\phi_c)$. That is:

$$R_g \exp(-j\phi_g) = R \exp(-j\phi) \quad \text{when gain factors and surface constants} \quad (156a)$$

appropriate for a ground reflection are used

$$R_c \exp(-j\phi_c) = R \exp(-j\phi) \quad \text{when gain factors and surface constants} \quad (156b)$$

appropriate for a counterpoise reflection are used

where the geometry used in calculating gain factors (Sec. 5.2.4) is dependent on the use of $H_{1,2}$ values in (106) that are appropriate for either ground or counterpoise reflection.

The total phase lag of the reflected ray relative to the direct ray for ground, ϕ_{Tg} , or counterpoise, ϕ_{Tc} , is given by:

$$\phi_{Tg,c} = (2\pi\Delta r_{g,c}/\lambda) + \phi_{g,c} + \phi_{kg,c} + \pi v_{g,c}^2/2 \quad \text{rad} \quad (157)$$

where $\Delta r_{g,c}$ is from (114), λ is from (10b), $\phi_{kg,c}$ is from (138), and $v_{g,c}$ is from (135). If there is no counterpoise, the last two terms of (157) may be neglected since they are the phase lag introduced by knife-edge diffraction over the counterpoise.

5.3 Line-of-Sight Transition Distance, d_0

The largest distance in the line-of-sight region at which diffraction is considered negligible is d_0 . In the IF-73 model, it was estimated using the distance at which the attenuation associated with a modified diffraction line is zero [14, p. 66]. The IF-73 d_0 is called d_d and in the IF-77 model is calculated as follows:

$$\theta_{h5} = 2 \sin^{-1} \left[\left(\frac{0.5}{5.1658} \right) \sqrt{d_{ML}/[fd_{L1}(d_{ML} - d_{L1})]} \right] \quad \text{rad} \quad (158)$$

where d_{ML} is from (43), f [MHz] is frequency, and d_{L1} is from Figure 5:

$$\theta_5 = \theta_{h5} - \tan^{-1} \left\{ [(h_1 - h_{L1})/d_{L1}] - d_{L1}/2a \right\} \quad (159)$$

where h_{L1} is from Figure 5, h_1 is from (21), and a is from 16.

$$h_{em2} = h_2 - \Delta h_{e2} \quad \text{km} \quad (160)$$

where h_2 is the aircraft altitude above msl (Fig. 2), and Δh_{e2} is from (25).

$$d_{L5} = -a \tan(\theta_5) + \sqrt{(a \tan \theta_5)^2 + 2a(h_{em2} - h_{L1})} \quad \text{km} \quad (161)$$

where a is from (16), and h_{L1} from Figure 5.

$$d_5 = d_{L5} + d_{L1} \quad \text{km} \quad (162)$$

$$\theta_{e5} = \text{Tan}^{-1} \left(\frac{h_{L1} - h_{em2}}{d_{L5}} - \frac{d_{L5}}{2a} \right) \quad \text{rad} \quad (163)$$

$$\theta_6 = \theta_{e1} + \theta_{e5} + (d_5/a) \quad \text{rad} \quad (164)$$

$$v_5 = 5.1658 \sin(0.5 \theta_6) \sqrt{fd_{L1}d_{L5}/d_5} \quad (165)$$

$$C_5 = \int_0^{v_5} \cos\left(\frac{\pi t^2}{2}\right) dt, \quad S_5 = \int_0^{v_5} \sin\left(\frac{\pi t^2}{2}\right) dt \quad (166)$$

where these are Fresnel Integrals [34, p. III-18].

$$f_5 = 0.5 \sqrt{[1 - (C_5 + S_5)]^2 + (C_5 - S_5)^2} \quad (167)$$

$$A_{K5} = -20 \log f_5 \quad \text{dB} \quad (168)$$

$$A_{r5} = A_F + M_F d_5 \quad \text{dB} \quad (169)$$

where A_F is from (54, 78) and M_F is from (55,77).

$$A_5 = \left\{ \begin{array}{l} A_{r5} \text{ if } W > 0.999 \\ A_{K5} \text{ if } W < 0.001 \\ (1 - W) A_{K5} + W A_{r5} \text{ otherwise} \end{array} \right\} \quad \text{dB} \quad (170)$$

where W is from (94), and

$$d_d = d_{ML} - A_{ML}(d_{ML} - d_5)/(A_{ML} - A_5) \quad \text{km} \quad (171)$$

where A_{ML} is from (95) and d_{ML} from (43).

Values estimated for d_o in IF-73 have been found to be too small when low antennas are used for both antennas. To correct this difficulty, d_o estimates in IF-77 are made using:

$$d_o = \left\{ \begin{array}{l} d_{L1} \text{ when } d_{L1} > d_d \\ d_{\lambda/6} \text{ when } d_{\lambda/6} > d_{L1} \text{ and } d_d \\ d_d \quad \text{otherwise} \end{array} \right\} \quad \text{km} \quad (172)$$

where d_{L1} is the horizon distance for the lower terminal (Fig. 5); $d_{\lambda/6}$ is the distance at which the path length difference, Δr , in a two-ray line-of-sight formulation is equal to $\lambda/6$ (λ is wave length); and d_d is the d_o of IF-73 [14, p. 66]. The distance $d_{\lambda/6}$ is the largest distance at which a free-space value is obtained in a two-ray model of reflection from a smooth earth with a reflection coefficient of -1. A value for $d_{\lambda/6}$ can be determined by the repetitive use of the line-of-sight formulation (Sec. 5.1) to define the Δr to distance relationship; i.e., (102) through (118).

5.4 Line-of-Sight Attenuation, A_{LOS}

Line-of-sight attenuation, A_{LOS} , is calculated as follows:

$$F_{fs} = \left\{ \begin{array}{l} 1 \text{ if lobing option is used and } \Delta r_g < 10\lambda \\ 1 \text{ if } \Delta r_g \leq 0.5 \lambda \quad \text{and} \\ \quad |g_D + R_{Tg} \exp(-j\phi_{Tg})| < g_D \\ 0 \quad \text{otherwise} \end{array} \right\} \quad (173)$$

where Δr_g is from (114), λ is from (10a), g_D is obtained using earth reflection geometry as indicated in Section 5.2.4, and $R_{Tg,c} \exp(-j\phi_{Tg})$ is from (119,157).

$$W_{RO} = |g_D + F_{fs} R_{Tg} \exp(-j\phi_{Tg}) + R_{Tc} \exp(-j\phi_{Tc})|^2 + 0.0001 g_D \quad (174)$$

$$A_{RO} = 10 \log (g_D^2 / W_{RO}) \quad \text{dB} \quad (175)$$

$$M_L = \frac{A_{ML} - A_o}{d_{ML} - d_o} \quad (176)$$

where A_{ML} is from (95), $A_o = A_{RO}$ from (175) evaluated for g_D and W_{RO} values that are applicable to $d = d_o$, d_{ML} is from (43), and d_o is from (172), and

$$A_{LOS} = \left\{ \begin{array}{l} A_{RO} \text{ if } d < d_o \\ A_o + M_L (d - d_o) \text{ if } d_o \leq d \leq d_{ML} \end{array} \right\} \text{ dB} \quad (177)$$

where d is from (118). The lobing option mentioned in (173) allows lobing due to ground reflections to be calculated for the first ten lobes inside the smooth-earth radio horizon [20, p. 99]. Note that lobing associated with reflection from the counterpoise is always included, but that (119b) gives $R_{Tc} = 0$ for (174) when there is no counterpoise (Sec. 5.2).

6. SCATTER REGION

The Rice et al. [34, Sec. 9] method to calculate attenuation for tropospheric scatter in IF-73 [14, Sec. A.4.4] is not applicable to paths that involve a very high antenna such as a satellite. This method was reformulated by Dr. George Hufford (DOC-BL, informal communication) to include geometric parameters associated with very high antennas where these parameters are determined using ray tracing techniques. The resulting formulation has been incorporated into IF-77 and may be summarized as follows:

$$U_{a1,2} = \left[\frac{(h_{L1,2} - h_{e1,2})}{a + h_{e,1,2}} + 2 \sin \left(\frac{d_{L1,2}}{2a} \right)^2 \right] / \sin \left(\frac{d_{L1,2}}{a} \right) \text{ rad} \quad (178)$$

where $h_{Lr1,2}$ is from (39, 47), a is from (16), the effective reflection surface elevation, h_r , is an input parameter, and $d_{L1,2}$ is from (41, 46).

$$d_s = d - d_{L1} - d_{L2} \quad \text{km} \quad (179)$$

where the great circle path distance, d , may be taken as an input parameter.

$$\theta_s = \theta_{a1} + \theta_{a2} + d_s/a \quad \text{rad} \quad (180)$$

$$d_{z1} = \left[\left(\frac{d_s}{2a} + \theta_{a2} \right) d_s + h_{L2} - h_{L1} \right] / \theta_s \quad \text{km} \quad (181)$$

where $h_{L1,2}$ are from (38, 48).

$$d_{z2} = d_s - d_{z1} \quad \text{km} \quad (182)$$

$$A_m = 157 (10^{-6}) \quad \text{per km} \quad (183)$$

$$dN = A_m - a^{-1} \quad \text{per km} \quad (184)$$

$$\gamma_e = N_s (10^{-6})/dN \quad \text{km} \quad (185)$$

where N_s is from (14).

$$z_{a1,2} = \frac{1}{2a} \left(\frac{d_{z1,2}}{2} \right)^2 + \theta_{a1,2} \left(\frac{d_{z1,2}}{2} \right) + h_{Lr1,2} \quad \text{km} \quad (186)$$

$$z_{b1,2} = \frac{1}{2a} d_{z1,2}^2 + \theta_{a1,2} d_{z1,2} + h_{Lr1,2} \quad \text{km} \quad (187)$$

$$Q_{o1,2} = A_m - dN \exp(-h_{Lr1,2}/\gamma_e) \quad (188)$$

$$Q_{a1,2} = A_m - dN \exp(-z_{a1,2}/\gamma_e) \quad (189)$$

$$Q_{b1,2} = A_m - dN \exp(-z_{b1,2}/\gamma_e) \quad (190)$$

$$Z_{a1,2} = \left[(7Q_{o1,2} + 6Q_{a1,2} - Q_{b1,2}) \frac{d_{z1,2}}{48} + \theta_{a1,2} \right] \frac{d_{z1,2}}{2} + h_{Lr1,2} \quad \text{km} \quad (191)$$

$$Z_{b1,2} = \left[(Q_{o1,2} + 2Q_{a1,2}) \frac{d_{z1,2}}{6} + \theta_{a1,2} \right] d_{z1,2} + h_{Lr1,2} \quad \text{km} \quad (192)$$

$$Q_{A1,2} = A_m - dN \exp(-Z_{a1,2}/\gamma_e) \quad (193)$$

$$Q_{B1,2} = A_m - dN \exp(-Z_{b1,2}/\gamma_e) \quad (194)$$

$$Z_{A1,2} = \left[(Q_{o1,2} + 2Q_{A1,2}) \frac{d_{z1,2}}{6} + \theta_{a1,2} \right] d_{z1,2} + h_{Lr1,2} \quad \text{km} \quad (195)$$

$$\theta_{A1,2} = \left(Q_{o1,2} + 4Q_{A1,2} + Q_{B1,2} \right) \frac{d_{z1,2}}{6} + \theta_{a1,2} \quad \text{rad} \quad (196)$$

$$\theta = \theta_{A1} + \theta_{A2} \quad \text{rad} \quad (197)$$

$$X_a = (Z_{A2} - Z_{A1})/\theta \quad \text{km} \quad (198)$$

$$d_{Z1} = d_{z1} + X_a \quad \text{km} \quad (199)$$

$$d_{Z2} = d_{z2} - X_a \quad \text{km} \quad (200)$$

$$h_v = (\theta_{A1} Z_{A2} + \theta_{A2} Z_{A1})/\theta \quad \text{km} \quad (201)$$

where h_v is the height of the scattering volume.

$$X_{A1,2} = (h_{e1,2} - h_{L1,2})^2 + 4(a + h_{e1,2})(a + h_{L1,2}) \sin \left(\frac{d_{L1,2}}{2a} \right)^2 \text{ km} \quad (202)$$

$$\ell_{1,2} = \sqrt{X_{A1,2}} + d_{Z1,2} \text{ km} \quad (203)$$

$$\ell = \ell_1 + \ell_2 \text{ km} \quad (204)$$

where ℓ is the total ray length.

$$\epsilon_1 = 0.031 - 2.32 (10^{-3}) N_S + 5.67 (10^{-6}) N_S^2 \quad (205)$$

$$\epsilon_2 = 0.0002 N_S^2 - 0.06 N_S + 6.6 \quad (206)$$

$$\gamma = 0.1424 \{1 + \epsilon_1 / \exp[(h_V/4)^6]\} \text{ per km} \quad (207)$$

$$S_e = 83.1 - \frac{\epsilon_2}{1 + 0.07716 h_V^2} + 20 \log[(0.1424/\gamma)^2 \exp(\gamma h_V)] \text{ dB} \quad (208)$$

where S_e is the scattering efficiency term.

$$s = (\ell_1 - \ell_2) / \ell \quad (209)$$

where s is the modulus of asymmetry.

$$A = (1 - s^2)^2 \quad (210)$$

$$\eta = \gamma \theta \ell / 2 \quad (211)$$

$$X_{V1} = (1 + s)^2 \eta \quad (212)$$

$$X_{V2} = (1 - s)^2 \eta \quad (213)$$

$$\kappa = 2\pi/\lambda \quad \text{per km} \quad (214)$$

where κ is the wave number and λ is from (10b).

$$\rho_{1,2} = 2\kappa\theta h_{e1,2} \quad (215)$$

where $h_{e1,2}$ are from (24).

$$q_{1,2} = \chi_{v1,2}^2 + \rho_{1,2}^2 \quad (216)$$

$$\begin{aligned} B_s = & 6 + 8s^2 \\ & + 8(1+s)\chi_{v2}^2\rho_2^2/q_2^2 \\ & + 8(1-s)\chi_{v1}^2\rho_1^2/q_1^2 \\ & + 2(1-s^2)(1+2\chi_{v1}^2/q_1)(1+2\chi_{v2}^2/q_2) \end{aligned} \quad (217)$$

$$C_s = 12 \left(\frac{\rho_1 + \sqrt{2}}{\rho_1} \right)^2 \left(\frac{\rho_2 + \sqrt{2}}{\rho_2} \right)^2 \left(\frac{\rho_1 + \rho_2}{\rho_1 + \rho_2 + 2\sqrt{2}} \right) \quad (218)$$

$$S_V = 10 \log \left(\frac{(A\eta^2 + B_s\eta)q_1q_2}{\rho_1^2\rho_2^2} + C_s \right) \quad \text{dB} \quad (219)$$

where S_V is the scattering volume term, and

$$A_s = S_e + S_V + 10 \log (\kappa\theta^3/\ell) \quad \text{dB} \quad (220)$$

where A_s is the tropospheric scatter attenuation.

7. TERRAIN ATTENUATION, A_T

The IF-77 formulation for terrain attenuation, A_T , may be summarized as follows:

$$A_T = \left[\begin{array}{l} A_{LOS} \text{ for } d < d_{ML} \\ \left. \begin{array}{l} A_d \text{ if } A_{sx} \geq A_{dx} \\ A_{sx} + \frac{A_{sx} - A_{ML}}{d_x - d_{ML}} (d - d_x) \text{ otherwise} \end{array} \right\} \text{ for } d_{ML} < d < d_x \\ \left. \begin{array}{l} \text{lesser of } A_d \text{ or } A_s \\ A_s \text{ once } A_s \text{ has been selected} \\ \text{for a shorter distance} \end{array} \right\} \text{ for } d_x < d \end{array} \right] \text{ dB} \quad (221)$$

where A_{LOS} is from (177), d is a specified parameter except in the LOS region where it is calculated via (118), A_d is from (100), $A_{sx} = A_s$ in (220) for $d = d_x$, $A_{dx} = A_d$ in (100) for $d = d_x$, A_{ML} is from (95), d_{ML} is from (43), and A_s is from (220). The distance, d_x , is the shortest distance just beyond the radio horizon ($d_{ML} < d$) at which $A_s > 20$ dB and $M_s \leq M_d$ where M_s is the slope of the A_s versus d curve as determined by successive A_s calculations (Sec. 6) and M_d is from (98).

8. FREE SPACE LOSS, L_{bf}

The IF-77 formulation [14, Sec. 8] free space basic transmission loss, L_{bf} , for use in (3), may be summarized as follows:

$$r_{WH} = \sqrt{(h_2 - h_1)^2 + 4(h_1 + a_0)(h_2 + a_0)[\sin(0.5d/a_0)]^2} \text{ km} \quad (222)$$

where $h_{1,2}$ are from (21), a_0 is from (15), and the great-circle path distance, d , is a starting parameter except for LOS paths where it is calculated from (118),

$$r_{L1,2} = \sqrt{(h_{1,2} - h_{L1,2})^2 + 4(h_{1,2} + a_0)(h_{L1,2} + a_0)[\sin(0.5d_{L1,2}/a_0)]^2} \text{ km} \quad (223)$$

where $h_{L1,2}$ are from (38,48)

$$r_{BH} = r_{L1} + r_{L2} + d_s \quad \text{km} \quad (224)$$

where d_s is from (179)

$$r = \text{greater of } \left\{ \begin{array}{l} r_o \text{ or } r_{WH} \text{ for LOS} \\ \text{or} \\ d \text{ or } r_{BH} \text{ otherwise} \end{array} \right\} \quad \text{km} \quad (225)$$

where r_o is from (112), and

$$L_{bf} = 32.45 + 20 \log (fr) \quad \text{dB} \quad (226)$$

where frequency, f [MHz], is a starting parameter [20, p. 82].

9. ATMOSPHERIC ABSORPTION

The formulation used to estimate median values for atmospheric absorption is similar to the IF-73 method [14, Sec. A.4.5]. Allowances are made for absorption due to oxygen and water vapor by using surface absorption rates and effective ray lengths where these ray lengths are lengths contained within atmospheric layers with appropriate effective thicknesses. Geometry associated with this formulation is shown in Figure 12 along with key equations relating geometric parameters. This geometry is used to calculate effective ray lengths applicable to the oxygen, r_{eo} , rain storm, r_{es} for Section 10.4, and water vapor, r_{ew} , layers for different path configurations. The rain storm is assumed to occur between the facility and its maximum LOS distance, d_{ML} from (43), so that only the facility horizon ray is considered in the calculation of r_{es} for beyond-the-horizon paths.

For line-of-sight paths, ($d \leq d_{ML}$) where d is a specified parameter except in the LOS region where it is calculated using (118), d_{ML} is from (43), the Figure 12 expressions are used to calculate effective ray lengths, $r_{eo,s,w}$, with $H_{\gamma 1,2} = H_{1,2}$ from (106), for earth, $a_{\gamma} = a_a$ from (104), and $\beta = \theta_{h1}$ from (115a).

Parameter values for $H_{\gamma 1}$ km, $H_{\gamma 2}$ km, and a_{γ} km and β are defined in the text for line-of-sight, single-horizon, and two-horizon paths.

$$A_t = \beta + 0.5 \pi$$

$$H_t = T_{eo,s,w} + a_{\gamma}$$

$$H_q = H_{\gamma 1} + a_{\gamma}$$

$$H_z = \text{lesser of } \{H_t \text{ or } H_{\gamma 2} + a_{\gamma}\}$$

When $H_{\gamma 1} < T_{eo,s,w}$

$$A_q = \sin^{-1} [(H_q \sin A_t) / H_z]$$

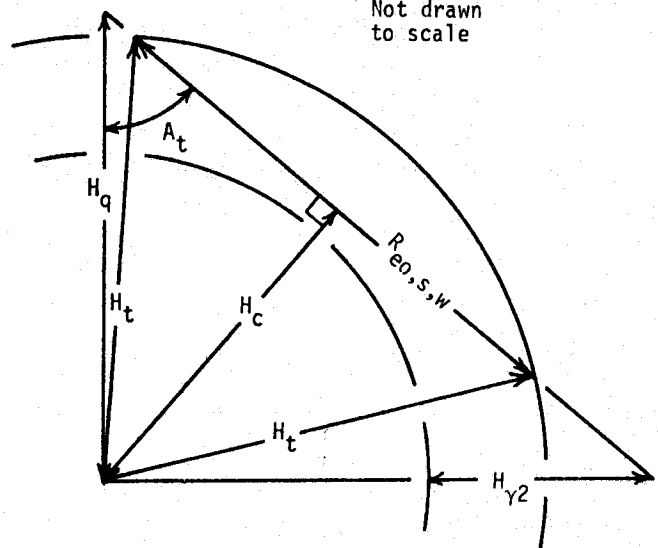
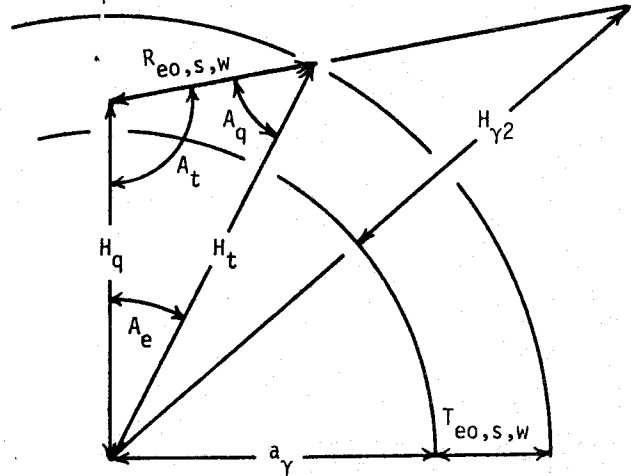
$$A_e = \pi - (A_t + A_q)$$

$$R_{eo,s,w} = \begin{cases} H_t - H_q & \text{if } A_q < 0.02 \text{ rad} \\ H_q \sin A_e / \sin A_q & \text{otherwise} \end{cases} \text{ km}$$

When $T_{eo,s,w} < H_{\gamma 1}$

$$H_c = H_q \sin A_t$$

$$R_{eo,s,w} = \begin{cases} 0 & \text{if } H_t \leq H_c \text{ or } A_t \geq \frac{\pi}{2} \\ 2 H_t \sin [\cos^{-1}(H_c / H_t)] & \text{otherwise} \end{cases} \text{ km}$$



Note: Values of $T_{eo,w}$ for oxygen and water vapor are taken as 3.25 and 1.36 km [12, Table A.2], respectively. The value of T_{es} used to estimate the in-storm ray length, R_{es} , for rain attenuation is dependent on the storm size (Section 10.4).

FIGURE 12. GEOMETRY ASSOCIATED WITH ATMOSPHERIC ABSORPTION CALCULATIONS.

For single horizon paths, ($d_{ML} < d \leq d_{L1} + d_{L01}$) where d_{L1} is from Figure 5 and d_{L01} is from (52), the Figure 12 expressions are used with one (R_{es}) or two ($R_{eo,w}$) sets of starting parameters and the $R_{eo,s,w}$'s obtained with these are called $r_{1eo,s,w}$ and $r_{2eo,w}$. In the calculation of $r_{1eo,s,w}$, $H_{\gamma 1}$ = lesser of (h_{e1} or h_{Lr1}) and $H_{\gamma 2}$ = greater of (h_{e1} or h_{Lr1}) where h_{e1} is from (24) and h_{Lr1} is from (39); $a_{\gamma} = a$ from (16) and $\beta = \theta_{e1}$ from (40) if $H_{\gamma 1} = h_{e1}$, otherwise $\beta = \theta_L$ from (42). In calculation for $r_{2eo,w}$, $H_{\gamma 1}$ = lesser of (h_{e2} from (24) or h_{Lr1}) and $H_{\gamma 2}$ = greater of (h_{e2} or h_{Lr2}) with $\beta = \theta_{e2}$ from (49) if $H_{\gamma 1} = h_{e2}$, otherwise $\beta = -\theta_L$. Values for $r_{eo,s,w}$ are then obtained using:

$$r_{es} = r_{les} \quad \text{km} \quad (227a)$$

$$r_{eo,w} = r_{1eo,w} + r_{2eo,w} \quad \text{km} \quad (227b)$$

For two-horizon paths ($d_{L1} + d_{L01} < d$), the Figure 12 expressions are also used with one (R_{es}) or two ($R_{eo,w}$) sets of input parameters. The results obtained are called $r_{1eo,s,w}$ and $r_{2eo,s,w}$, where (227) is used to determine $r_{eo,s,w}$ values. In calculations for $r_{1eo,s,w}$, $H_{\gamma 1}$ = lesser of $\{h_{e1}$ or h_v from (201)\}, $H_{\gamma 2}$ = greater of $\{h_{e1}$ or $h_v\}$, $\beta = \theta_{e1}$ if $H_{\gamma 1} = h_{e1}$, otherwise $\beta = -\tan^{-1}\theta_{A1}$ where θ_{A1} is from (196). In calculations for $r_{2eo,s,w}$, $H_{\gamma 1}$ = lesser of $\{h_v$ or $h_{e2}\}$, $H_{\gamma 2}$ = greater of $\{h_v$ or $h_{e2}\}$, $a_{\gamma} = a$ and $\beta = \theta_{e2}$ if $H_{\gamma 1} = h_{e2}$, otherwise $\beta = -\tan^{-1}\theta_{A2}$ where θ_{A2} is from (196).

Surface absorption rates for oxygen and water vapor, $\gamma_{oo,w}$ are used with effective ray lengths, $r_{eo,w}$ to obtain an estimate for atmospheric absorption, A_a ; i.e.,:

$$A_a = \gamma_{oo} r_{eo} + \gamma_{ow} r_{ew} \quad \text{dB} \quad (228)$$

Values for $\gamma_{oo,w}$ are obtained by interpolating between values taken from the Rice et al. curves [34, p. 3-7].

10. VARIABILITY

Total variability, $Y_{\Sigma}(q)$, for (1) is calculated from:

$$Y_{\Sigma}(q) = \pm \sqrt{Y_e^2(q) + Y_{\pi}^2(q) + Y_r^2(q) + Y_I^2(q)} \quad \text{dB} \quad (229)$$

+ for $q \leq 0.5$

- otherwise

where $Y_e(q)$ is the variability associated with long-term (hour-to-hour) power fading (Sec. 10.1), $Y_{\pi}(q)$ is short-term (within-the-hour) fading associated with surface reflection multipath (Sec. 10.2) and tropospheric multipath (Sec. 10.3), $Y_r(q)$ is rain attenuation fading (Sec. 10.4), and $Y_I(q)$ is ionospheric scintillations (Sec. 10.5). When the long-term (hourly median) time availability option [20, p. 103] is selected, short-term fading is neglected (i.e., $Y_{\pi}(q) = Y_r(q) = Y_I(q) = 0$) and the resulting variability may be regarded as the variability of hourly medians. Since $Y_{\pi}(0.5) = Y_r(0.5) = Y_I(0.5) = 0$, $Y_{\Sigma}(0.5)$ does not change when short-term fading is neglected. For $q \leq 0.98$, $Y_r(q) = 0$; i.e., rain attenuation only occurs during 2 percent of the time. Furthermore, $Y_I(q) = 0$ except for earth/satellite paths that pass through the ionosphere which is at an altitude of about 350 km.

10.1. Long-Term Power Fading, $Y_e(q)$

The variability associated with long-term (hourly median) power fading for (229) is designated $Y_e(q)$ where q is the time availability parameter of Section 2.1 and the sign associated with $Y_e(q)$ values is such that the positive values associated with $q \leq 0.5$ will decrease transmission loss or increase received power levels. All long-term variability options [20, p. 103] use an effective distance, d_e [34, Secs. 10, III-6, III-7] which is calculated as follows:

$$d_{qs} = 65 (100/f)^{1/3} \quad \text{km} \quad (230)$$

where f [MHz] is frequency:

$$d_q = d_{Lq} + d_{qs} \quad \text{km} \quad (231)$$

where d_{Lq} is a total smooth earth horizon distance determined by ray tracing (Sec. 3) with $N_s = 329$ in (17) which would correspond to a 9000 km effective earth radius [34, p. 4-4]

$$d_e = \left\{ \begin{array}{l} 130d/d_q \text{ for } d \leq d_q \\ 130 + d - d_q \text{ otherwise} \end{array} \right\} \text{ km} \quad (232)$$

where d is the great-circle path distance and is a specified parameter except in the LOS region where it is calculated via (118). Key parameters, $g(0.1 \text{ or } 0.9, f)$, $V(0.5)$ and $Y_0(0.1 \text{ or } 0.9)$ for the long-term variability normally used are determined as follows:

$$g(0.1, f) = \left\{ \begin{array}{l} 0.21 \sin[5.22 \log(f/200)] + 1.28 \text{ for } 60 \leq f \leq 1600 \text{ MHz} \\ 1.05 \text{ for } f > 1600 \text{ MHz} \end{array} \right\} \quad (233a)$$

$$g(0.9, f) = \left\{ \begin{array}{l} 0.18 \sin[5.22 \log(f/200)] + 1.23 \text{ for } 60 \leq f \leq 1600 \text{ MHz} \\ 1.05 \text{ for } f > 1600 \text{ MHz} \end{array} \right\} \quad (233b)$$

$$f_2 = f_\infty + (f_m - f_\infty) \exp\left(-c_2 d_e^{n_2}\right) \quad (234)$$

and

$$\left. \begin{array}{l} V(0.5) \\ Y_0(0.1) \\ -Y_0(0.9) \end{array} \right\} = \left[c_1 d_e^{n_1} - f_2 \right] \exp\left(-c_3 d_e^{n_3}\right) + f_2 \text{ dB} \quad (235)$$

where the values used for the parameters c_1 , c_2 , c_3 , n_1 , n_2 , n_3 , f_m , and f_∞ depend on whether $V(0.5)$ [34, Table III.5, Climate 1], $Y(0.1)$ [34, Table III.3, all hours all year], or $Y(0.9)$ [34, Table III.4, all hours all year] is calculated. This selection is based on a recommended model [11, p. 19] that was tested against air/ground data [10, Sec. 4.3]. However, other options such as different time blocks (Sec. 10.1.1), climates (Sec. 10.1.2), or a mix performed to meet particular

conditions (Sec. 10.6) may be used. The key parameters from (233,235) or elsewhere (Secs. 10.1.1, 10.1.2) are used to obtain the final long-term variability distribution as follows:

$$Y(0.1 \text{ or } 0.9) = g(q = 0.1 \text{ or } 0.9, f) Y_0(q = 0.1 \text{ or } 0.9) \quad \text{dB} \quad (236)$$

$$Y(q) = \left\{ \begin{array}{l} cY(0.1) \text{ for } q < 0.5 \\ 0 \text{ for } q = 0.5 \\ cY(0.9) \text{ for } q > 0.5 \end{array} \right\} \quad \text{dB} \quad (237)$$

where c values for the q desired are selected from Tables [15, p. 34].

$$f_{\theta h} = \left\{ \begin{array}{l} 0.5 - \pi^{-1} \tan^{-1} \left[20 \log (32\theta_{h1}) \right] \text{ for LOS} \\ \text{paths with } \theta_{h1} > 0 \\ 1 \text{ otherwise} \end{array} \right\} \quad (238)$$

where θ_{h1} is from (115)[13, p. 8; 34, p. III.43].

$$Y_{eI}(q) = f_{\theta h} Y(q) \quad \text{dB} \quad (239)$$

$$V_e(0.5) = f_{\theta h} V(0.5) \quad \text{dB} \quad (240)$$

$$Y_T = L_b(0.5) - [L_{bf} - V_e(0.5) - 20 \log (R_{Tg} + R_{Tc})] \quad \text{dB} \quad (241)$$

where $L_b(0.5)$ is from (2), L_{bf} is from (226), $R_{Tg,c}$ are from (119).

$$A_{YI} = \left\{ \begin{array}{l} 0 \text{ if lobing option [20, p. 99] is used} \\ \text{and aircraft is within 10 lobes of} \\ \text{its radio horizon} \\ (L_{bf} - 3) - [L_{br} - Y_{eI}(0.1)] \text{ otherwise} \end{array} \right\} \quad (242)$$

where L_{br} is from (3).

$$A_Y = \left\{ \begin{array}{ll} 0 & \text{if } A_{YI} \leq 0 \\ 10 & \text{if } A_{YI} \geq 10 \\ A_{YI} & \text{otherwise} \end{array} \right\} \quad (243)$$

$$Y_e(q < 0.1) = \left\{ \begin{array}{l} \text{lesser of } [Y_{eI}(q) \text{ or } Y_T] \text{ for lobing} \\ \text{lesser of } [Y_{eI}(q) \text{ or} \\ L_{br} + A_Y - (L_{bf} - c_Y)] \\ \text{otherwise} \end{array} \right\} \text{ dB} \quad (244)$$

where c_Y is 6, 5.8, and 5 dB for q values of 0.0001, 0.001, and 0.01, respectively,

$$Y_e(q \geq 0.1) = Y_{eI}(q) \quad \text{dB} \quad (245)$$

10.1.1 Time Blocks

Long-term variability options for IF-77 include variabilities appropriate for the time blocks shown in Table 1 [20, p. 103]. These blocks and seasonal groupings are used to describe the diurnal and seasonal variations in a continental temperate climate [34, Sec. III.7.1]. They are incorporated into (235) by selecting appropriate constants from Rice et al. [34, Tables III.2, III.3, and III.4]. The expressions for $g(0.1, f)$ and $g(0.9, f)$ given in (233) are used for time block variabilities.

If a combination of time blocks is appropriate, various distributions can be mixed (Sec. 10.6).

10.1.2 Climates

Options to use various climates are included in IF-77 [20, p. 103]; i.e., (1) equatorial, (2) continental sub-tropical, (3) maritime sub-tropical, (4) desert, (5) mediterranean, (6) continental temperate, (7a) maritime temperate overland, (7b) maritime temperate oversea, and (8) polar. The formulation used is based on algebraic expressions fitted to modified versions of curves provided in CCIR Report 238-4 [7] by Hufford and Longley [DOC-BL, informal communication; 15, Sec. 4.3; 29, Sec. 4.4.25] and may be summarized as follows:

TABLE 1. TIME BLOCK RANGES [34, Sec. III.7.1]

NO.	MONTHS	HOURS
1	Nov. - Apr.	0600 - 1300
2	Nov. - Apr.	1300 - 1800
3	Nov. - Apr.	1800 - 2400
4	May - Oct.	0600 - 1300
5	May - Oct.	1300 - 1800
6	May - Oct.	1800 - 2400
7	May - Oct.	0000 - 0600
8	Nov. - Apr.	0000 - 0600
Summer	May - Oct.	ALL-HOURS
Winter	Nov. - Apr.	ALL-HOURS

$$\left. \begin{array}{l} V(0.5) \\ Y_o(0.1) \\ -Y_o(0.9) \end{array} \right\} = \frac{(d_e/b_1)^2}{1 + (d_e/b_1)^2} \left[c_1 + \frac{c_2}{1 + [(d_e - b_2)/b_3]^2} \right] \text{ dB} \quad (246)$$

where d_e is from (232), and appropriate values for the b_1 , b_2 , b_3 , c_1 , and c_2 are used [15, p. 33].

$$g(0.1, f) = \left\{ \begin{array}{l} 1 \text{ for all climates except 2, 4, and 6,} \\ 0.18 \sin [5 \log (f/200)] + 1.06 \\ \quad \text{for } 60 \leq f \leq 1500 \text{ MHz in Climates 2 and 6,} \\ 1 \text{ suggested for } 60 \leq f \leq 200 \text{ MHz in Climate 4,} \\ 0.10 \sin [5 \log (f/200)] + 1.02, \\ \quad \text{for } 200 \leq f \leq 1500 \text{ MHz in Climate 4,} \\ 0.93 \text{ for } f > 1500 \text{ MHz in Climates 2, 4, and 6} \end{array} \right\} \quad (247a)$$

$$g(0.9, f) = \left. \begin{array}{l} 1 \text{ for all climates except 6,} \\ 0.13 \sin [5 \log (f/200)] + 1.04 \\ \text{for } 60 \leq f \leq 1500 \text{ MHz in Climate 6,} \\ 0.92 \text{ for } f > 1500 \text{ MHz in Climate 6} \end{array} \right\} \quad (247b)$$

where f [MHz] is an IF-77 input parameter [20, p. 82]. When one of these climate options is selected, the key parameters obtained from (246,247) are used in (236,240). If a mixture of two or more climates is appropriate, various distributions can be mixed (Sec. 10.6).

10.2 Surface Reflection Multipath

Multipath associated with reflections from the earth's surface is considered as part of the short-term (within the hour) variability for line-of-sight paths, and is used only when the time availability option for "instantaneous levels exceeded" is selected [20, p. 103]. Contributions associated with both specular and diffuse reflection components may be included though the specular component is not allowed to make a full contribution when it is also used in determining the median levels (e.g., when lobing option is selected [20, p. 99]). These contributions are incorporated into the variability part of the model via the relative power level, W_R , which is used to compute $Y_\pi(q)$ for (229) as shown in Section 10.3. Formulas used to calculate W_R may be summarized as follows:

$$F_{AY} = \left. \begin{array}{l} 1 \text{ if } A_Y \leq 0 \\ 0.1 \text{ if } A_Y \geq 9 \\ 0.5 [1.1 + 0.9 \cos (\pi A_Y / 9)] \text{ otherwise} \end{array} \right\} \quad (248)$$

where A_Y is from (243),

$$F_{\Delta r} = \left\{ \begin{array}{l} \left\{ \begin{array}{l} 1 \quad \text{for } \Delta r_g > 10\lambda \\ 0 \quad \text{otherwise} \end{array} \right\} \quad \left\{ \begin{array}{l} \text{for lobing} \\ \text{option [20, p. 99]} \end{array} \right\} \\ \left\{ \begin{array}{l} 1 \quad \text{for } \Delta r_g \geq \lambda/2 \\ 0.1 \quad \text{for } \Delta r_g \leq \lambda/6 \\ \text{otherwise} \\ \frac{1.1 - 0.9 \cos[3\pi(\Delta r_g - \lambda/6)/\lambda]}{2} \end{array} \right\} \quad \text{otherwise} \end{array} \right\} \quad (249)$$

where Δr_g is from (114b) and λ is from (10b)

$$R_s = R_{Tg} (F_{AY} F_{\Delta r}) \quad (250)$$

where R_s^2 is the relative contribution of specular reflection to surface reflection multipath power, and R_{Tg} is from (119a), R_d from (129) may be expressed as:

$$R_d = R_{Tg} \left(\frac{F_{doh}}{F_{oh} D_v} \right) \quad (251)$$

where R_d^2 is the relative contribution of diffuse reflection to surface reflection multipath power, F_{doh} is from (128), F_{oh} is from (127), and D_v is from (122),

$$W_R = \left\{ \begin{array}{l} \left((R_s^2 + R_d^2) / g_D^2 \right) \text{ for LOS } (d \leq d_{ML}) \\ 0 \quad \text{otherwise} \end{array} \right\} \quad (252)$$

where d is the path length obtained from (118) for LOS paths, d_{ML} is from (43), and g_D is from (141).

10.3 Tropospheric Multipath

Tropospheric multipath is caused by reflections from atmospheric sheets or elevated layers, or additional direct (nonreflected) wave paths [2; 9, Sec. 3.1], and may be present when antenna directivity is sufficient to make surface reflections negligible. It is considered as part of the short-term (within the hour) variabil-

ity used only when the time availability option for "instantaneous levels exceeded" is selected [20, p. 103], and incorporated into the variability part of the model via the relative power level, W_a . This is used to compute $Y_{\pi}(q)$ for (229) as shown in the latter part of this section. The formulation for W_a may be summarized as follows:

$$F = \left\{ \begin{array}{l} 10 \log (f r_{ew}^3) - 84.26 \text{ for } d \leq d_{ML} \\ \text{and is not calculated otherwise} \end{array} \right\} \text{ dB} \quad (253)$$

where frequency, f [MHz] is an input parameter [20, p. 82], r_{ew} is calculated as indicated on Figure 12, d is from (118) for $d \leq d_{ML}$, and d_{ML} is from (43).

$$K_{LOS} = \left\{ \begin{array}{l} 40 \text{ dB for } F \leq 0.14 \\ -20 \text{ dB for } F \geq 18.4 \\ \text{otherwise obtained from curves} \end{array} \right\} \text{ dB} \quad (254)$$

where curves for the Nakagami-Rice probability distribution [34, p. V-8] are used by selecting the "K" (which becomes K_{LOS}) that corresponds to a " $Y_{\pi}(0.99)$ " of $-F$

$$M_{Ka} = (-20 - K_{ML}) / 0.02618 \quad \text{dB/rad} \quad (255)$$

where K_{ML} is K_{LOS} evaluated at the maximum LOS range (i.e., $d = d_{ML}$).

$$K_t = \left\{ \begin{array}{l} K_{LOS} \text{ for } d \leq d_{ML} \\ -20 \text{ for } \theta_s > 0.02618 \text{ rad} \\ K_{ML} + M_{Ka} \theta_s \text{ otherwise} \end{array} \right\} \text{ dB} \quad (256)$$

where θ_s is the scattering angle from (180) and is negative in the LOS region.

$$W_a = 10^{-K_t/10} \quad (257)$$

Relative powers W_a and W_R from (252) are combined to determine K , which is the ratio in decibels between the steady component (e.g., direct ray), and the Rayleigh fading component (e.g., surface reflection and tropospheric multipath) using:

$$K = -10 \log (W_R + W_a) \quad \text{dB} \quad (258)$$

The Nakagami-Rice probability distribution for $Y_{\pi}(q)$ of (229) is then selected from the Rice et al. curves [34, p. V-8] by using K .

10.4 Rain Attenuation

The rain attenuation model used in IF-77 is largely based on material in informal papers by C. A. Samson (DOC-BL) on "Radio Propagation Through Precipitation" and "Rain Rate Distribution Curves." This discussion is a shortened version of the description previously provided [15, Sec. 4.4], and the maps and tables provided there are not repeated here.

Two options for rain attenuation are available in IF-77. The first is for use in a "worst case" type analysis where a particular rainfall attenuation rate is assumed for the in-storm path length, and the additional path attenuation associated with rain is simply taken as the product of this attenuation rate (in dB/km) and the in-storm ray length [20, p. 94]. This ray length is determined in accordance with the method discussed in step 4 of option two.

Option two involves computer input of rain zone (which determines a rainfall rate distribution) and storm size [20, p. 94]. Storm size (diameter or long dimension) is assumed to be one of three options: 5, 10, or 20 km (corresponding approximately to a relatively small, average, or very large thunderstorm). The maximum distance used in calculating path attenuation with this option is the storm size since it is assumed that only one storm is on the path at a time. The process used to include rain attenuation estimates in IF-77 for this option may be summarized as follows:

1. Determine point rain rates. Point rain rates (rate at a particular point of observation) not exceeded for specific fractions of the time are determined for the rain zone of interest [15, p. 38].

2. Determine path average rain rates. Each point rain rate resulting from step 1 is converted to a path average rain rate by using linear interpolation to obtain a multiplying factor [15, p. 39].

3. Determine attenuation rate. For each path average rain rate resulting from step 2, an attenuation rate $A_{rr}(q)$ [dB/km] is determined using linear interpolation between the values previously determined for various rainfall rates and frequency [15, p. 40].

4. Determine the in-storm ray length. First, the length of the direct ray r_{es} that is within T_{es} of the earth's surface is determined from (227) by using the method described in Section 9 where T_{es} is taken as the storm size; i.e., storm height is assumed to be equivalent to storm diameter. Then, the final in-storm ray length, r_s , is calculated using:

$$r_s = \left\{ \begin{array}{ll} T_{es} & \text{if } r_{es} \geq T_{es} \\ r_{es} & \text{otherwise} \end{array} \right\} \quad (259)$$

5. Determine rain attenuation values. Values for the attenuation, $A_r(q)$ for a particular fraction of time are calculated using

$$A_r(q) = \left\{ \begin{array}{ll} 0 & \text{for } q \leq 0.98 \\ A_{rr}(q)r_s & \text{otherwise} \end{array} \right\} \text{ dB} \quad (260)$$

where $A_{rr}(q)$ values come from step 3 and the value for r_s is from step 4. Distributions of rain attenuation are zero for $q \leq 0.98$ [15, p. 38].

6. Combine rain attenuation variability with other variabilities. Variability for rain attenuation, $Y_r(q)$, is related to the distribution of rain attenuation by:

$$Y_r(q) = -A_r(q) \quad (261)$$

It is combined with other variabilities in (229).

10.5 Ionospheric Scintillation

Variability associated with ionospheric scintillation, $Y_I(q)$ for (229), for paths that pass through the ionosphere (i.e., on earth/satellite paths) at an altitude of about 350 km is included in IF-77. This variability may be specified directly by the selection of a scintillation index group or by using a weighted mixture of distributions where the weighting factors are estimated for specific problems [20, p. 91; 15, Sec. 4.5]. Provisions are included to allow $Y_I(q)$ to change with earth facility latitude when a geostationary satellite is involved and the earth facility locations are along the subsatellite meridian. When this provision is used, $Y_{136}(q)$ is obtained from previously prepared 136 MHz data [15, p. 45] and $Y_I(q)$ is calculated as follows:

$$n = \left\{ \begin{array}{l} 1 \quad \text{for } \theta_{FL} \leq 17^\circ \text{ or } \theta_{FL} \geq 52^\circ \\ 1 + (\theta_{FL} - 17)/7 \quad \text{for } 17^\circ < \theta_{FL} < 24^\circ \\ 2 \quad \text{for } 24^\circ < \theta_{FL} < 45^\circ \\ 1 + (52 - \theta_{FL})/7 \quad \text{for } 45^\circ < \theta_{FL} < 52^\circ \end{array} \right\} \quad (262)$$

where θ_{FL} is the magnitude of the earth facilities latitude in degrees, and

$$Y_I(q) = (136/f)^n Y_{136}(q) \quad \text{dB} \quad (263)$$

Even though this scaling factor is built into the programs that utilize IF-77, only minor program modifications would be required to use other simple scaling methods. In addition, the distribution mixing methods of Section 10.6 could be used to create $Y_I(q)$'s applicable to specific situations.

10.6 Mixing Distributions

Subroutines have been incorporated into the IF-77 computer programs to allow the distributions that characterize portions of the variability associated with a particular model component to be mixed in order to obtain the total variability for that component. For example, different fractions of the time may be characterized

by signal level distributions associated with different ionospheric scintillation groups; and, with these subroutines, they can be weighted and combined (mixed) to obtain the total variability associated with ionospheric scintillations (Sec. 10.5).

The process of mixing N cumulative variability distributions may be summarized as follows:

1. Select M (ten or more) levels of variability $V_1, \dots, V_i, \dots, V_M$ that cover the entire range of the transmission loss (or power available, etc.) values involved.
2. Determine the fraction of time (weighting factor) for which each distribution is applicable; i.e., $W_1, \dots, W_j, \dots, W_N$.
3. Determine the time availability (fraction of time during which a distribution is applicable that a specific level of transmission loss is not exceeded) for each distribution at the selected levels; i.e., $q_{11}, \dots, q_{ij}, \dots, q_{MN}$.
4. Calculate time availabilities for the mixed distribution that corresponds to the variability levels selected, i.e.:

$$\begin{aligned}
 q_1 &= q_{11}W_1 + \dots + q_{1j}W_j + \dots + q_{1N}W_N \\
 &\cdot \\
 &\cdot \\
 &\cdot \\
 q_i &= q_{i1}W_1 + \dots + q_{ij}W_j + \dots + q_{iN}W_N \\
 &\cdot \\
 &\cdot \\
 &\cdot \\
 q_M &= q_{M1}W_1 + \dots + q_{Mj}W_j + \dots + q_{MN}W_N
 \end{aligned}
 \tag{264}$$

This process is the same as the one used by Rice et al. [34, Sec. III.7.2] to combine transmission loss distributions for time blocks to obtain distributions for summer and winter. It is, also, essentially the same as the method recommended by Whitney et al. [38, p. 1099; 39, Sec. 6] to combine distributions of fading associated with various ionospheric scintillation index groups (Sec. 10.5).

When this process is used to mix distributions of long-term variability, the required variability functions are obtained from:

$$V_c(q) = [V(0.5) + Y(q)]|_c \quad \text{dB} \quad (265)$$

where ...|_c indicates that the V(0.5) and Y(q) are appropriate for the conditions (e.g., time block or climate) associated with a particular value of the subscript c. For example, V(0.5) and Y(q) values for different climates can be obtained by using (247) with (236, 237) and mixing can be used to estimate variability for areas near a border between two different climate types. After mixing, Y(q) values needed for (239) may be obtained by using:

$$Y(q) = V(q) - V(0.5) \quad \text{dB} \quad (266)$$

where all variables in (266) are associated with the resulting mixed distribution. Similarly, when mixing variabilities associated with ionospheric scintillation,

$$Y_{Ic}(q) = Y_I(q)|_c \quad \text{dB} \quad (267)$$

and the distribution resulting from the mixing is taken as Y_I(q) for later calculations.

11. SUMMARY

The IF-77 electromagnetic wave propagation model was discussed, and references were provided so that more information on specific items could be obtained. A brief description of the model provided in Section 2 is followed by a systematic discussion of model components. Readers with a further interest in IF-77 are encouraged to obtain a copy of the "Applications Guide for Propagation and Interference Analysis Computer Programs (0.1 to 20 GHz)" [20].

APPENDIX

ABBREVIATIONS, ACRONYMS, AND SYMBOLS

This list includes most of the abbreviations, acronyms, and symbols used in this report. Many are similar to those previously used [14, 15, 20, 34]. The units given for symbols in this list are those required by or resulting from equations as given in this report and are applicable except when other units are specified.

In the following list, the English alphabet precedes the Greek alphabet, letters precede numbers, and lower-case letters precede upper-case letters. Miscellaneous symbols and notations are given after the alphabetical items.

a	Effective earth radius [km] calculated from (16).
a_a	An adjusted effective earth radius [km] shown in Figure 8, from (104).
a_0	Actual earth radius, 6370 km, to about three significant figures.
a_γ	An effective earth radius [km] used in Figure 12, and defined for different path types in Section 9.
$a_{1,2}$	Effective earth radii [km], from (62).
$a_{3,4}$	Effective earth radii [km], from (63).
A	A parameter used in tropospheric scatter calculations, from (210).
A_a	Atmospheric absorption [dB], from (228).
A_A	Combined diffraction attenuation [dB] at $d = d_A$, from (97).
A_d	Attenuation [dB] associated with diffraction beyond the horizon, from (100).
A_{d0}	Intercept [dB] for the beyond-the-horizon combined diffraction attenuation line, from (99).
A_{dx}	A_d [dB] at d_x , discussed after (221).
$A_{e,q,t}$	Angles [rad] defined and used in Figure 12 only.

A_F	Attenuation line intercept [dB] of rounded earth diffraction for path F-0-ML (Figure 7), from (54,78).
A_I	Effective area [dB-sq m] of an isotropic antenna, from (9).
A_{KA}	Knife-edge diffraction attenuation [dB] for path F-0-A (Figure 7), from (93).
A_{KML}	Knife-edge diffraction attenuation [dB] for path F-0-ML (Figure 7), from (87).
A_{K5}	Knife-edge diffraction attenuation [dB] at d_5 , from (168).
A_{LOS}	Line-of-sight attenuation [dB], from (177).
A_m	A parameter [km] used in tropospheric scatter calculations, from (183).
A_{ML}	Combined diffraction attenuation [dB] at d_{ML} , from (95).
A_o	A_{R0} [dB] at d_o , from (175).
A_O	Attenuation line intercept [dB] of rounded earth diffraction path O-A (Figure 7), from (54,78).
A_p	Rounded earth diffraction attenuation [dB] for path p, from (54,78).
A_{rA}	A_{rF} [dB] at d_A , from (85).
A_{rF}	Rounded earth diffraction attenuation [dB] for path F-0-A (Figure 7), from (85).
A_{rML}	A_{rF} [dB] at d_{ML} , from (85).
A_{r0}	Rounded earth diffraction attenuation [dB] for path O-A (Figure 7) at distance d_{LSA} , from (86).
A_{R0}	Attenuation [dB] in the line-of-sight region where the diffraction effects associated with terrain are negligible ($d < d_o$), from (175).
$A_r(q)$	Attenuation [dB] due to rain for a fraction of time q, from (260).
$A_{rr}(q)$	Attenuation rate [dB/km] associated with rain and a fraction of time q, (Sec. 10.4, Step 3).
A_{r5}	A_{rF} [dB] at d_5 , from (169).
A_s	Forward scatter attenuation [dB], from (220).

A_{sx}	A_s [dB] at d_x , discussed after (221).
A_T	Terrain attenuation [dB], from (221).
A_Y	A conditional adjustment factor [dB] used to prevent available signal powers from exceeding levels expected for free-space propagation by unrealistic amounts, from (243).
A_{YI}	An initial value of A_Y [dB], from (242).
$A_{3,4}$	Rounded earth diffraction attenuations [dB], from (76).
A_5	Combined diffraction attenuation [dB], at d_5 , from (170).
$b_{1,2,3}$	Long-term variability parameters with values previously provided [15, p. 33], used in (246).
B	A parameter used in the $G_{\bar{h}_{1,2}}$ formulation of (83).
$B_{N1,2}$	Parameters used in rounded earth diffraction formulation, from (79).
B_s	A parameter used in forward scatter formulation, from (217).
$B_{1,2,3,4}$	Parameters used in the rounded earth diffraction formulation, from (68).
c	A parameter used in (237) with values taken from tables [15, p. 34].
$c_{e,h,v}$	Phase of plane earth reflection coefficient relative to π for elliptical, horizontal, and vertical polarization.
c_Y	A variability limiting parameter [dB] used in (244) and defined just after (244).
$c_{1,2,3}$	Long-term variability parameters for (234,235,246) that are discussed following (235).
C_e	An exponential atmosphere parameter, from (18).
C_s	A parameter used in tropospheric scatter calculations, from (218).
$C_{v,g,c,5}$	A Fresnel integral [34, III-18], for (92,137,167).
d	Great-circle distance between facility and aircraft. For line-of-sight paths, it is calculated via (118).
dB	Decibel, $10 \log$ (dimensionless ratio of powers).
dB _i	Antenna gain in decibels greater than isotropic.

dB/km	Attenuation [dB] per unit length [km].
dB-sq m	Units for effective area in terms of decibels greater than an effective area of 1 square meter; i.e., $10 \log$ (area in square meters).
dBW	Power in decibels greater than 1 watt.
dB-W/sq m	Units of power density in terms of decibels greater than 1 watt per square meter; i.e., $10 \log$ (power density expressed in watts per square meter).
dN	A parameter [per km] used in tropospheric scatter calculations, from (184).
d_A	A facility-to-aircraft (Figure 7) distance [km], from (96).
d_C	Counterpoise diameter [km], a model input parameter [20, p. 88, <u>FACILITY ANTENNA COUNTERPOISE DIAMETER</u>].
d_d	Initial estimate of d_0 , from (171).
d_e	Effective distance [km], from (232).
d_h	A distance [km] used in facility horizon determination, from (35).
d_{LE1}	An initial value for the facility horizon distance [km] that is based on effective earth radius geometry, and shown in Figure 4. It may be specified [20, p. 90] or calculated as indicated in Figure 5, from (33,36).
d_{LM}	Maximum distance [km] for which the facility-to-aircraft path has a common horizon, from (45).
$d_{L01,2}$	Smooth earth horizon distances [km] for path 0-A (Figure 7), from (52,53).
d_{Lp}	Total horizon distances [km] for path p, from (59).
$d_{Lp1,2}$	Radio horizon distances [km] for path p, from (52,53).
d_{Lq}	Smooth earth horizon distances [km] determined via ray tracing (Sec. 3) over a 9000-km (4860 n mi) earth, discussed after (231).
d_{LR2}	Horizon distance for aircraft shown in Figure 4 and discussed preceding (43).

d_{Ls}	Total smooth earth horizon distance [km], from (28).
d_{LsA}	The sum of the smooth earth distances of path 0-A (Figure 7), from (88).
$d_{LsE1,2}$	A smooth earth horizon distance [km] for the facility or aircraft that is based on effective earth radius geometry, from (26).
$d_{LsR1,2}$	Smooth earth horizon distances determined via ray tracing (Sec. 3.1), and shown in Figure 3.
$d_{Ls1,2}$	Smooth earth horizon distances determined, from (27).
d_{L1}	Facility-to-horizon distance [km], determined as shown in Figure 5, from (41).
d_{L2}	Horizon distance for aircraft, from (46).
d_{L5}	A distance [km], calculated from (161).
d_{ML}	Maximum line-of-sight distance [km] shown in Figure 4, from (43).
d_o	The largest distance [km] in the line-of-sight region at which diffraction effects associated with terrain are considered negligible, from (172).
d_q	A distance [km], calculated from (231).
d_{qs}	Distance [km] beyond the radio horizon at which diffraction and scatter attenuation are approximately equal for a smooth earth, from (230).
d_s	Distance [km] between horizons, from (179).
d_{sL}	Smooth earth horizon distance [km] for the obstacle height as shown in Figure 6, from (44).
d_x	A distance [km] just beyond the radio horizon where $A_s \geq 20$ dB and $M_s \leq M_d$, discussed after (221).
$d_{z1,2}$	Distances [km] used in tropospheric scatter calculations, from (181,182).
$d_{z1,2}$	Distances [km] used in tropospheric scatter calculations, from (199,200).

$d_{3,4}$	Distances [km] used in rounded earth diffraction calculation, from (60,61).
d_5	A distance [km] calculated from (162).
$d_{\lambda/6}$	The largest distance [km] at which a free-space value of basic transmission loss is obtained in two-ray model of reflection from a smooth earth with an effective reflection coefficient of -1. This occurs when the path length difference, Δr from (114), is equal to $\lambda/6$.
DOC-BL	United States <u>D</u> epartment of <u>C</u> ommerce, <u>B</u> oulder <u>L</u> aboratories.
DOT	United States <u>D</u> epartment of <u>T</u> ransportation.
D/U(q)	Desired-to-undesired signal ratio [dB] exceeded for at least a fraction q of the time. These values may represent instantaneous levels or hourly median levels depending upon the time availability option selected [20, p. 103] and are calculated via (11).
D_v	Divergence factor, from (122).
$D_{1,2}$	Distances [km] shown in Figure 8 and calculated via (109).
e	2.718281828.
eq.	Equation.
exp()	Exponential; e.g., $\exp(2) = e^2$ or $R \exp(-j\phi) = R e^{-\sqrt{-1}\phi}$ is a phasor with magnitude R and a lag of ϕ radians.
EIRP	<u>E</u> quivalent <u>i</u> sotropically <u>r</u> adiated <u>p</u> ower [dBW] as defined by (7).
EIRPG	EIRP [dBW] increased by the main beam <u>g</u> ain [dBi] of the receiving antenna as in (6).
f	Frequency [MHz], an input parameter [20, p. 82].
fss	<u>F</u> acility <u>s</u> ite <u>s</u> urface (Figure 2).
$f_{c1,2}$	A parameter used in G_h weighting factor and calculated from (81).
$f_{g,c,v,5}$	Knife-edge diffraction loss factors determined using Fresnel integrals, from (137,92,167).
$f_{m,2,\infty}$	Parameters used in the normally used variability formulation and discussed following (235).
f_{oh}	Elevation angle correction factor, from (238).

F	Fade margin [dB], from (253).
FAA	<u>F</u> ederal <u>A</u> viation <u>A</u> dmistration.
F_{AY}	A specular reflection reduction factor associated with A_Y , from (248).
$F_{d\sigma h}$	Reflection reduction factor associated with diffuse reflection and surface roughness [5,Figure 4], from (128).
F_{fs}	A factor calculated from (173).
F_r	Reflection reduction factor associated with ray lengths, from (123).
$F_{X1,2}$	Parameters [dB] calculated from (75).
$F_{1,2}$	Parameters [dB] calculated from (74).
$F_{\Delta r}$	Reflection reduction factor associated with Δr , from (249).
$F_{\sigma h}$	Specular reflection reduction factor associated with surface roughness, from (127).
$g(0.1, f)$ or $g(0.9, f)$	Frequency gain factor, from (233,247).
$g_{D,R}$	Voltage gain [V/V] factors associated with direct and reflected rays, from (141,142).
$g_{D1,2}$	Voltage gain [V/V] of terminal antennas in the direction of the direct ray (Figure 11), relative to main beam gain.
$g_{hD1,2}$	Voltage gain [V/V] similar to $g_{D1,2}$, but specifically for horizontal polarization.
$g_{hR1,2}$	Voltage gain [V/V] similar to $g_{R1,2}$, but specifically for horizontal polarization.
$g_{Rg,c}$	Gain factors used in (119) for earth or counterpoise reflected rays, from (149).
g_{Rh}	Gain factor for the reflected ray and horizontal polarization, from (144).
g_{Rv}	Gain factor for the reflected ray and vertical polarization, from (143).
$g_{R1,2}$	Voltage gain [V/V] of terminal antennas in the direction of the reflected ray (Figure 11) relative to main beam gain, from (140).

$g_{vD1,2}$	Voltage gain [V/V] similar to $g_{D1,2}$, but specifically for vertical polarization.
$g_{vR1,2}$	Voltage gain [V/V] similar to $g_{R1,2}$, but specifically for vertical polarization.
GHz	Gigahertz (10^9 Hz).
$G_{ET,R}$	Gain [dBi] of the transmitting or receiving antenna at an appropriate elevation angle, from (4).
$G_{\bar{h}1,2}$	Values [dB] for the residual height gain function, from (83).
$G_{\bar{h}F1,2}$	$G_{\bar{h}p1,2}$ [dB] for path F-0-ML (Figure 7), from (56,84).
$G_{\bar{h}O1,2}$	$G_{\bar{h}p1,2}$ [dB] for path 0-A (Figure 7), from (56,84).
$G_{\bar{h}p1,2}$	Values [dB] for the weighted residual height gain function (Sec. 4.2) for path p, from (56,84).
$G_{NT,R}$	Normalized gain of the transmitting or receiving antenna at appropriate elevation angle in decibels greater than the main beam (G_T or G_R), from (145).
$G_{R1,2}$	Gains [dB] $g_{R1,2}$ expressed in decibels, from (139).
$G_{T,R}$	Gain [dBi] of the transmitting or receiving main beam for (4,6,7).
$G_{W1,2}$	Weighting factor, from (82).
$G_{1,2,3,4}$	Parameters [dB] calculated from (71).
h	Ray height [km] above msl used in (17).
h_c	Height [km] of facility counterpoise above ground at the facility site, an input parameter [20, p. 88].
h_e	An effective height [km], from (34).
h_{em2}	Effective aircraft altitude [km] above msl, from (160).
$h_{ep1,2}$	Effective antenna heights [km] for path p, from (50,51).
$h_{e1,2}$	Effective antenna height [km] above h_r (Figure 3), from (24), and shown in Figure 3.

h_{fc}	Height [km] of the facility antenna above its counterpoise (Figure 2).
h_{LE1}	An initial value for the facility horizon elevation [km] above msl that is based on effective earth radius geometry (Figure 4). It may be specified [20, p. 90, <u>HORIZON OBSTACLE HEIGHT</u>] or calculated as indicated in Figure 5.
h_{Lr1}	Height of facility horizon [km] above the reflecting surface (Figure 6), from (39).
h_{Lr2}	Height [km] of aircraft horizon above the reflecting surface, from (47).
$h_{L1,2}$	Horizon elevations [km] above the msl, from (38,48).
h_r	Elevation [km] of effective reflecting surface above msl (Figure 2), an input parameter [20, p. 83, <u>EFFECTIVE REFLECTION SURFACE ELEVATION</u>].
$h_{r1,2}$	Actual antenna elevations above reflecting surface elevation, from (20), and shown in Figure 2.
h_{sm1}	Height [km] of facility site surface above msl (Figure 2), an input parameter [20, p. 101, <u>TERRAIN ELEVATION</u>].
h_{s1}	Height [km] of facility antenna above the facility site surface (Figure 2), an input parameter [20, p. 81].
h_v	Height [km] of the common volume above the reflection plane for scatter calculations, from (201).
$h_{1,2}$	Antenna elevations [km] above msl, from (21) and shown in Figure 2, h_2 is an input parameter [20, p. 80].
$\bar{h}_{1,2}$	Parameters calculated from (80).
$H_{c,q,t,z}$	Heights [km] defined and illustrated in Figure 12.
$H_{1,2}$	Antenna elevation [km] above the reflecting surface (Figure 8), from (106).
$H'_{1,2}$	Antenna elevations [km] from (110) and shown in Figure 8.
$H_{1/3}$	Significant wave height [20, p. 99] used in (125).
$H_{\gamma 1,2}$	Heights [km] used in Figure 12 and defined for different path types in Section 9.
i	An index for specific transmission loss levels used in the distribution mixing process (Section 10.6). It has values from 1 to M.

IF-73	<u>ITS-FAA-1973</u> propagation model.
IF-77	<u>ITS-FAA-1977</u> propagation model.
ITS	<u>Institute for Telecommunication Sciences.</u>
j	$\sqrt{-T}$ as in (154) or index (1 to N) for specific transmission loss distributions used in the distribution mixing process (Sec. 10.6).
k_a	An adjusted earth radius factor, from (103).
K	The ratio [dB] between the steady component of received power and the Rayleigh fading component that is used to determine the appropriate Nagagami-Rice distribution [34, p. V-8] for $Y_{\pi}(q)$, from (258).
$K_{d1,2,3,4}$	Rounded earth diffraction parameters, from (65).
$K_{F1,2}$	Rounded earth diffraction parameters, from (67).
K_{LOS}	K_t values in the line-of-sight region, from (254).
K_{ML}	K values at the radio horizon; i.e., K_{LOS} at $d = d_{ML}$, from (254).
K_t	K value associated with tropospheric multipath, from (256).
$K_{1,2,3,4}$	Rounded earth diffraction parameters, from (66).
λ	Total ray length [km] in scatter calculation, from (204).
log	Common (base 10) logarithm.
\log_e	Natural (base e) logarithm.
$\lambda_{1,2}$	Ray lengths [km] to the cross-over point of the common volume in tropospheric scatter calculations, from (203).
LOS	<u>Line-of-sight.</u>
$L(q)$	Transmission loss [dB] values <u>not</u> exceeded during a fraction q of the time. These values may represent instantaneous levels depending upon the time availability option selected (Sec. 10), and are calculated using (1).
L_{bf}	Basic transmission loss [dB] for the free space, from (226).

L_{br}	A reference level of basic transmission loss [dB], from (3).
$L_b(0.5)$	Median basic transmission loss [dB], from (2).
L_{gp}	Loss [dB] in path antenna gain used in and discussed after (3); current model assumes $L_{gp} = 0$.
mhos	Unit of conductance or siemens.
msl	<u>Mean sea level</u> .
M	Number of transmission loss levels used in mixing distributions which is also the final value for the index i (Sec. 10.6).
MHz	Megahertz (10^6 Hz).
M_d	Slope [dB/km] of combined diffraction attenuation line for beyond-the-horizon, from (98).
M_F	Slope [dB/km] of rounded earth diffraction attenuation line for path F-0-ML (Figure 7), from (55,77).
M_{Ka}	Slope [dB/km] of the K value line used just beyond the radio horizon, from (255).
M_L	Slope [dB/km] of the diffraction attenuation line used just inside the radio horizon, from (176).
M_0	Slope [dB/km] of rounded earth diffraction line attenuation for path 0-A (Figure 7), from (55,77).
M_p	Slope [dB/km] of rounded earth diffraction attenuation line for path p, from (55,77).
M_s	Slope [dB/km] of successive scatter attenuation points (A_s versus d line), discussed after (221).
n	A power used in the ionospheric scintillation frequency scaling factor (Sec. 10.5), from (262).
$n_{1,2,3}$	Parameters for (234,235) that are discussed following (235).
N	Refractivity [N-units] for a height h in an exponential atmosphere, from (17).
N	Number of distributions to be mixed which is also the final value for the index j (Sec. 10.6).
N-units	Units of refractivity [3, Sec. 1.3] corresponding to 10^6 (refractive index -1).

NTIA	<u>N</u> ational <u>T</u> elecommunications and <u>I</u> nformation <u>A</u> dministration.
N_0	Minimum monthly mean surface refractivity (N-units) referred to msl, an input parameter [20, p. 94].
N_s	Minimum monthly mean surface refractive (N-units) at effective reflection surface, calculated from N_0 via (14).
$P_a(q)$	Power [dBW] that is available at the terminal of an ideal (loss-less) receiving antenna for at least a fraction q of the time, from (5).
P_{TR}	Total power [dBW] radiated from the transmitting antenna, used in (7).
q	Dimensionless fraction of time used in time availability specification; e.g., in $L_b(0.1)$, $q = 0.1$ implies a time availability of 10 percent.
$q_{1,2}$	Parameters used in tropospheric scatter calculations, from (216).
$q_{1,i,M}$	Time availabilities for mixed distributions that correspond to specific transmission loss levels, from (264).
$q_{11,ij,MN}$	Time availabilities for each transmission loss level (index i) of each transmission loss distribution (index j) involved in the distribution mixing distribution (Sec. 10.6).
$Q_{a1,2}$	Parameters used in tropospheric scatter calculations, from (189).
$Q_{A1,2}$	Parameters used in tropospheric scatter calculations, from (193).
$Q_{b1,2}$	Parameters used in tropospheric scatter calculations, from (190).
$Q_{B1,2}$	Parameters used in tropospheric scatter calculations, from (194).
$Q_{o1,2}$	Parameters used in tropospheric scatter calculations, from (188).
r	Ray length [km] used in the calculation of free space loss, from (225).
r_{BH}	Ray length [km] for beyond-the-horizon paths, from (224).
r_c	A distance [km], from (131).
$r_{eo,s,w}$	Effective ray lengths [km] for attenuation associated with oxygen absorption (r_{eo}), rain storm attenuation (r_{es}), and water vapor absorption (r_{ew}), from (227).

$r_{L1,2}$	Antenna to horizon ray lengths [km] for airless earth, from (223).
r_o	Direct ray length [km] shown in Figure 8, from (112).
r_s	In-storm ray length [km] used in rain attenuation calculation, from (259).
r_{WH}	Within-the-horizon ray length [km] for airless earth, from (222).
$r_{1,2}$	Segments of reflected ray path shown in Figure 8 and components of r_{12} , from (120).
r_{12}	Reflected ray path length [km] as shown in Figure 8, from (113).
$r_{1eos,w}$ and $r_{2eo,w}$	Partial effective ray lengths [km] for oxygen layer, rain storm or water vapor layer or calculated using the relationships given in Figure 12, as indicated in Section 9.
R	Magnitude of complex plane earth reflection coefficient, from (155).
RAYTRAC	A computer subroutine used to trace a ray through an exponential atmosphere [14, p. 182].
$R_{c,g}$	Magnitude of effective reflection coefficient for counterpoise or ground reflection, from (156).
R_d	Diffuse component of surface reflection multipath, from (129, 251).
$R_{e,h,v}$	Magnitudes of complex plane earth reflection coefficients for elliptical, horizontal, and vertical polarization.
$R_{eo,s,w}$	Partial effective ray lengths [km] inside oxygen layer, rain-storm or water vapor layer, as calculated as shown in Figure 12.
R_r	A parameter used in the calculation of the divergence factor, from (121).
R_s	Specular component of surface reflection multipath, from (250).
$R_{Tg,c}$	Magnitude of adjusted effective reflection coefficient for earth or counterpoise reflection, from (119).
s	Modules of asymmetry used in tropospheric scatter calculations, from (209).

SHF	<u>S</u> uper <u>H</u> igh <u>F</u> requency [3 to 30 GHz].
\sin^{-1}	Inverse sine with principal value.
S_e	Scattering efficiency term [dB] used in tropospheric scatter calculations, from (208).
$S_R(q)$	Power density at receiving antenna locations [dB-W/sq m] for at least a fraction q of the time, from (8).
$S_{v,g,c,5}$	A Fresnel integral [34, p. III-18], for (92,137,167).
S_V	Scattering volume term [dB] of tropospheric scatter calculations, from (219).
T	A parameter defined and used in (83), the $G_{\bar{h}}$ formulation.
T	Relaxation time [μ s] used in the calculation of water surface constants, for (151).
\tan^{-1}	Inverse tangent [rad] with principal value.
TWIRL	A program name [20, p. 9].
$T_{eo,s,w}$	Storm height or layer thickness (Figure 12) used in attenuation calculations for oxygen absorption (T_{eo}), rain storm attenuation (T_{es}), or water vapor absorption (T_{ew}).
UHF	<u>U</u> ltra- <u>H</u> igh <u>F</u> requency [300 to 3000 MHz].
v	Knife-edge diffraction parameter, from (90).
$v_{g,c,5}$	Knife-edge diffraction parameters used to determine $f_{g,c,5}$, from (135,165).
VHF	<u>V</u> ery <u>H</u> igh <u>F</u> requency [30 to 300 MHz].
V/V	Volts per volt.
V(0.5)	A parameter [dB], from (235,246).
$V_c(q)$	Variability for specific climate or time block, from (265).
$V_e(0.5)$	Variability adjustment term [dB], from (240).
$V_{1,i,M}$	Variability levels ($V_1, \dots, V_i, \dots, V_M$) used in mixing distributions (Sec. 10.6).
W	A weighting factor used in combining knife-edge and rounded earth diffraction attenuations, from (94).
W	Watts.

W_a	A relative power level for the Rayleigh fading component associated with tropospheric multipath, from (257).
W_R	A relative power level for the Rayleigh fading component associated with surface reflection multipath, from (252).
W_{RO}	A relative power level associated with the ray optics formula-tion used in the line-of-sight region, from (174).
$W_{1,2}$	Parameters, from (72).
$W_{1,j,N}$	Weighting factors ($W_1, \dots, W_j, \dots, W_N$) used in mixing distri-butions (Sec. 10.6).
x	A parameter, from (64).
X_a	A parameter used in tropospheric scatter calculations, from (198).
$X_{A1,2}$	Parameters used in tropospheric scatter calculations, from (202).
$X_{v1,2}$	Parameters used in tropospheric scatter calculations, from (212,213).
$X_{1,2,3,4}$	Parameters [km], from (69,70).
$Y_{1,2}$	Parameters [dB], from (73).
$Y(q)$	Variability [dB greater than median] of hourly median received power about its median, from (237).
$Y(0.1)$ or $Y(0.9)$	A reference variability level of hourly median received power about its median and is used to calculate the other percentiles, from (236).
Y_c	A complex parameter used in the calculation of the plane earth reflection coefficient, from (153).
$Y_{DU}(q)$	Total variability [dB greater than median] of D/U about its median, $Y_{DU}(0.5) = 0$, where q is the fraction of time for which a particular value is exceeded.
$Y_e(q)$	Effective variability [dB greater than median] of hourly median received power about its median, from (244,245).
$Y_{eI}(q)$	Initial value of $Y_e(q)$, from (239).

$Y_I(q)$	Variability [dB] associated with ionospheric scintillation, from (263).
$Y_{Ic}(q)$	$Y_I(q) _c$ for a particular distribution to be used in the mixing process to obtain resultant $Y_I(q)$, from (267).
$Y_r(q)$	Variability [dB greater than median] associated with rain attenuation, from (261).
$Y_o(0.1)$ or $Y_o(0.9)$	A reference variability level used to calculate $Y(0.1)$ or $Y(0.9)$, from (235,246).
Y_T	A top limiting level when the calculations are in the lobing mode in the line-of-sight region, from (241).
Y_v	A parameter from (133).
$Y_{136}(q)$	Variability [dB] for (263) that is associated with ionospheric scintillation at 136 MHz [15, p. 45].
$Y_\pi(q)$	Variability [dB greater than median] of received power used to describe short-term (within-the-hour) fading associated with multipath where q is the fraction of time during which a particular level is exceeded (Sec. 10.3).
$Y_\Sigma(q)$	Total variability [dB greater than median] of received power about its median, $Y_\Sigma(0.5) = 0$, where q is the fraction of time for which a particular value is exceeded, from (229). These values may represent instantaneous levels or hourly median levels depending upon the time availability option selected [20, p. 103, <u>TIME AVAILABILITY OPTIONS</u>].
z	A parameter from (102).
$z_{a1,2}$	Parameters used in tropospheric scatter calculations, from (186).
$z_{b1,2}$	Parameters used in tropospheric scatter calculations, from (187).
$z_{1,2}$	Parameters [km], from (107).
$z_{a1,2}$	Parameters used in tropospheric scatter calculations, from (191).
$z_{A1,2}$	Parameters used in tropospheric scatter calculations, from (195).
$z_{b1,2}$	Parameters used in tropospheric scatter calculations, from (192).

α	An angle [rad] shown in Figure 8, from (111).
β	An angle [rad] used in Figure 12 and defined for different path types in Section 9.
γ	A parameter [per km] used in tropospheric scatter calculations, from (207).
γ_e	A parameter in tropospheric scatter calculations, from (185).
$\gamma_{oo,w}$	Surface absorption rates [dB/km] for oxygen or water vapor for (228).
δ	A parameter used in the calculation of the surface roughness factors, from (126).
Δh	Terrain parameter [km] used to characterize terrain irregularity. It is a model input parameter [20, p. 101, <u>TERRAIN PARAMETER</u>].
$\Delta h_{a1,2}$	Adjusted effective altitude correction factors, from (105).
Δh_d	Interdecile range of terrain heights [m] above and below a straight line fitted to elevations above msl; estimated from (124) which is based on previous work [26, eq. 3].
$\Delta h_{e1,2}$	Effective altitude correction factors, from (25).
Δh_m	Δh expressed in meters for (124).
ΔN	Refractivity gradient [N-units/km] used in defining exponential atmospheres, from (19).
Δr	Path length difference [km] for rays shown in Figure 8 ($r_{12} - r_0$), from (101,114).
$\Delta r_{g,c}$	Δr [km] for earth or counterpoise reflection, from (114).
ϵ	Dielectric constant, model input parameter [20, p. 99, <u>SURFACE TYPE OPTIONS</u>].
ϵ_c	Complex dielectric constant, from (152).
ϵ_0	Dielectric constant representing the sum of electronic and atomic polarizations. For water, $\epsilon_0 = 4.9$ in (150,151).
ϵ_s	Static dielectric constant for water [15, p. 26].
$\epsilon_{1,2}$	Parameters used in tropospheric scatter calculations, from (205,206).

η	A parameter used in tropospheric scatter calculations, from (211).
θ	Scattering angle [rad] used in tropospheric scatter calculations. It is the angle between transmitter horizon to common volume ray and the common volume to receiver horizon ray as both leave their crossover point, from (197).
$\theta_{a1,2}$	Angles [rad], from (178).
$\theta_{A1,2}$	Angles [rad] used in tropospheric scatter calculations; angles between the common volume horizontal and the horizon to the common volume rays as they leave their crossover point, from (196).
θ_{ce}	An angle [rad] shown in Figure 9, from (130).
θ_{eE1}	An initial value for the facility horizon elevation angle [rad] that is based on effective earth radius geometry, and is shown in Figure 4. It may be specified [20, p. 90, <u>HORIZON OBSTACLE ABOVE HORIZONTAL AT FACILITY</u>] or calculated as indicated in Figure 5.
$\theta_{esR1,2}$	Smooth earth horizon ray elevation angle [rad] at the appropriate terminal as determined from ray tracing (Sec. 3.1). Illustrated in Figure 3.
$\theta_{es1,2}$	Final value for smooth earth horizon ray elevation angle [rad] at the appropriate terminal, from (30).
θ_{e1}	Elevation angle [rad] of horizon from the facility, from (40).
θ_{e2}	Elevation angle [rad] of aircraft horizon ray shown in Figure 6, from (49).
θ_{e5}	An angle [rad], from (163).
θ_{FL}	Magnitude of earth facility latitude [deg] for (262).
$\theta_{g1,2}$	Elevation angles [rad] of the ground reflected rays at the terminal antennas, from (148).
$\theta_{h1,2}$	Parameter [rad] used to calculate $\theta_{H1,2}$, from (115).
θ_{h5}	An angle [rad], from (158).
$\theta_{H1,2}$	Direct ray elevation angles [rad] at the terminal antennas, from (147).

$\theta_{kg,c}$	Angles [rad] used in (135), from (132,134).
θ_L	Elevation angle [rad] of horizon-to-aircraft ray at facility horizon (Figure 4), from (42).
$\theta_{L1,2}$	Horizon elevation angle [rad] adjustment terms, from (146).
θ_0	Central angle [rad], from (117).
$\theta_{r1,2}$	Angles [rad] used in (148), from (116).
θ_s	An angle [rad], from (180).
$\theta_{sR1,2}$	Smooth earth horizon ray elevation angles [rad] that are obtained using ray tracing horizon distances with an effective earth formulation and shown in Figure 3, from (23).
$\theta_{s1,2}$	Central angles [rad] below the smooth earth terminal to horizon distances, from (29).
θ_v	Diffraction angle [rad] for the O-A path (Figure 7), from (89).
$\theta_{1,2}$	Angles [rad] shown in Figure 8, from (108).
$\theta_{3,4}$	Angles [rad], from (57,58).
θ_5	An angle [rad], from (159).
θ_6	An angle [rad], from (164).
κ	Wave number [per km], from (214).
λ	Wavelength [km], from (10).
λ_m	Wavelength [m], from (10).
μs	Microseconds [10^{-6} sec].
π	The constant 3.141592654.
$\rho_{1,2}$	Parameters used in tropospheric scatter calculations, from (215).
σ	Surface conductivity [mho/m], a model input parameter [20, p. 99, <u>SURFACE TYPE OPTIONS</u>].

σ_h	The root-mean-square deviation [m] of terrain and terrain clutter within the limits of the first Fresnel zone in the dominant reflecting plane; estimated from (125), which is based on previous work [26, Annex 3, eqs. 3.6a, 3.6b].
σ_i	Ionic conductivity [mho/m] for water, [15, p. 26].
ϕ	Phase advance associated with complex earth reflection coefficient used in (155).
$\phi_{g,c}$	Phase shift [rad] of effective reflection coefficient for earth or counterpoise reflection, used in (156).
$\phi_{kg,c}$	Knife-edge diffraction phase shift [rad] for earth or counterpoise reflection, from (138).
$\phi_{Tg,c}$	Total phase shift [rad] of effective reflection coefficient for earth or counterpoise reflection, from (157).
ψ	Grazing angle shown in Figures 8 and 9.
$ c$	Expression evaluated for specific conditions such as climate or time block in (267).

REFERENCES

- [1] Ames, L. A., P. Newman, and T. F. Rogers (1955), VHF tropospheric overwater measurements far beyond the radio horizon, Proc. IRE 43, No. 10, 1369-1373.
- [2] Barnett, W. T. (1972), Multipath propagation at 4, 6, and 11 GHz, Bell Sys. Tech. J. 51, No. 2, 321-361.
- [3] Bean, B. R., and E. J. Dutton (1968), Radio Meteorology (Dover Publications, Inc., New York, N.Y.).
- [4] Bean, B. R., and G. D. Thayer (1959), CRPL Exponential Reference Atmosphere, NBS Monograph 4 (NTIS, PB-174 987)².
- [5] Beard, C. I. (1961), Coherent and incoherent scattering of microwaves from the ocean, IRE Trans. Ant. Prop. AP-9, No. 5, 470-483.
- [6] Bremmer, H. (1949), Terrestrial Radio Waves (Elsevier Pub. Co., New York, N.Y.).
- [7] CCIR (1982), Propagation data required for trans-horizon radio-relay systems, Report 238-4, XVth Plenary Assembly, Geneva (Intl. Telecom. Union, Geneva).
- [8] CCIR (1982), VHF, UHF, and SHF propagation curves for the aeronautical mobile service, Rec. 528-2, XVth Plenary Assembly, Geneva (Intl. Telecom. Union, Geneva).
- [9] Dougherty, H. T. (1967), Microwave fading with airborne terminals, ESSA Tech. Report IER 58-ITSA 55 (NTIS, N-70-73581)².
- [10] Gierhart, G. D., A. P. Barsis, M. E. Johnson, E. M. Gray, and F. M. Capps (1971), Analysis of air-ground radio wave propagation measurements at 800 MHz, Office of Telecommunications Report OT/TRER 21 (NTIS, COM-75-10830/AS)².
- [11] Gierhart, G. D., R. W. Hubbard, and D. V. Glen (1970), Electrospace planning and engineering for the air traffic environment, Department of Transportation Report FAA-RD-70-71 (NTIS, AD 718 447)².
- [12] Gierhart, G. D., and M. E. Johnson (1969), Transmission loss atlas for select aeronautical service bands from 0.125 to 15.5 GHz, ESSA Technical Report ERL 111-ITS 79 (GPO, \$1.25)¹.
- [13] Gierhart, G. D., and M. E. Johnson (1972), UHF transmission loss estimates for GOES, Office of Telecommunications Technical Memo. OT TM-109 (NTIS, COM-73-10339)².
- [14] Gierhart, G. D., and M. E. Johnson (1973), Computer programs for air/ground propagation and interference analysis, 0.1 to 20 GHz, DOT Report FAA-RD-73-103 (NTIS, AD 770 335)².
- [15] Gierhart, G. D., and M. E. Johnson (1978), Propagation model (0.1 to 20 GHz) extensions for 1977 computer programs, DOT Report FAA-RD-77-129 (NTIS, ADA 055605)².

- [16] Hartman, W. J., Editor (1974), Multipath in air traffic control frequency bands, DOT Report FAA-RD-74-75, I & II (NTIS, AD/A-006, 267 and 268)².
- [17] IEEE (1970), Special issue on air traffic control. Proc. IEEE 58, No. 3.
- [18] Janes, H. B. (1955), An analysis of within-the-hour fading in the 100- to 1000-Mc transmission, J. Res. NBS 54, No. 4, 231-250.
- [19] Johnson, M. E., and G. D. Gierhart (1978), Aerospace propagation prediction capabilities associated with the IF-77 model, AGARD Conf. Proc. No. 238, Paper 48 (NTIS, AD-A063 792/6GA)².
- [20] Johnson, M. E., and G. D. Gierhart (1978), Applications guide for propagation and interference analysis computer programs (0.1 to 20 GHz), DOT Report FAA-RD-77-60 (NTIS, ADA 053242)².
- [21] Johnson, M. E., and G. D. Gierhart (1979), Comparison of measured data with IF-77 propagation model predictions, DOT Report FAA-RD-79-9 (NTIS, ADA-076508)².
- [22] Johnson, M. E., and G. D. Gierhart (1980), An atlas of transmission loss for 0.125 to 15.5 GHz, DOT Report FAA-RD-80-1 (NTIS, ADA 088153)².
- [23] Kerr, D. E. (1964), Propagation of short radio waves, MIT Radiation Lab. Series 13 (Boston Tech. Pub., Inc., Lexington, Mass.).
- [24] Longley, A. G., and R. K. Reasoner (1970), Comparison of propagation measurements with predicted values in the 20 to 10,000 MHz range, ESSA Technical Report ERL 148-ITS 97 (NTIS, AD 703 579)².
- [25] Longley, A. G., R. K. Reasoner, and V. L. Fuller (1971), Measured and predicted long-term distributions of tropospheric transmission loss, Office of Telecommunications Report OT/TRER 16 (NTIS, COM-75-11205)².
- [26] Longley, A. G., and P. L. Rice (1968), Prediction of tropospheric radio transmission loss over irregular terrain, a computer method-1968, ESSA Tech. Report ERL 79-ITS 67 (NTIS, AD 676 874)².
- [27] McCormick, K. S., and L. A. Maynard (1971), Low angle tropospheric fading in relation to satellite communications and broadcasting, IEEE ICC Record 7, No. 12, 18-23.
- [28] Medhurst, R. G. (1965), Rainfall attenuation of centimeter waves: comparison of theory and measurement, IEEE Trans. Ant. and Prop. AP-13, No. 4, 550-564.
- [29] Military Handbook (1977), Facility Design for Tropospheric Scatter (Transhorizon Microwave System Design, DOD MIL-HDBK-417)³.
- [30] Millington, G. (1957), The concept of the equivalent radius of the earth in tropospheric propagation, Marconi Rev. 20 No. 126, 79-93.
- [31] Millington, G. (1958), Propagation at great heights in the atmosphere, Marconi Rev. 21 No. 131, 143-160.

- [32] Norton, K. A., L. E. Vogler, W. V. Mansfield, and P. J. Short (1955), The probability distribution of the amplitude of a constant vector plus a Rayleigh-distributed vector, Proc. IRE 43, No. 10, 1354-1361.
- [33] Reed, H. R., and C. M. Russell (1964), Ultra High Frequency Propagation (Boston Tech. Publishers, Lexington, Mass.).
- [34] Rice, P. L., A. G. Longley, K. A. Norton, and A. P. Barsis (1967), Transmission loss predictions for tropospheric communications circuits, NBS Tech. Note 101, I and II revised (NTIS, AD 687 820 and AD 687 821)².
- [35] Riblet, H. J., and C. B. Baker (1948), A general divergence formula, J. Appl. Phys. 19, 63-70.
- [36] Saxton, J. A., and J. A. Lane (1952), Electrical properties of sea water, Wireless Engr. 29, 6-7.
- [37] Thayer, G. D. (1967), A rapid and accurate ray tracing algorithm for a horizontally stratified atmosphere, Radio Sci. 1, (New Series), No. 2, 249-252.
- [38] Whitney, H. E., J. Aarons, and R. S. Allen (1972), Estimation of the cumulative amplitude probability distribution function of ionospheric scintillations, Radio Sci. 7, No. 12, 1095-1104.
- [39] Whitney, H. E., J. Aarons, and D. R. Seemann (1971), Estimation of the cumulative amplitude probability distribution function of ionospheric scintillations, Air Force Cambridge Res. Labs. Report AFCRL-71-0525, Cambridge, Mass.

¹Copies of this report were sold for the indicated price by the Superintendent of Documents, U. S. Government Printing Office, Washington, DC 20402, and may still be available.

²Copies of these reports are sold by the National Technical Information Services (NTIS), 5285 Port Royal Road, Springfield, VA 22161. Order by indicated accession number.

³Copy of this handbook may be ordered from the Commanding Officer, Naval Publications and Forms Center, ATTN: NPFC 3015, 5801 Tabor Avenue, Philadelphia, PA 19120; telephone: 215-697-3321.

